

Simple and Accurate Oscillation Probabilities for Three Coupled Neutrinos Propagating in Matter

Mikkel B. Johnson

Los Alamos National Laboratory, Los Alamos, NM 87545

Leonard S. Kisslinger

Department of Physics, Carnegie-Mellon University, Pittsburgh, PA 15213

Within a conventional Hamiltonian description, we find accurate closed-form expressions for the oscillation probabilities of three coupled neutrinos propagating in matter. Subtle cancelations that occur in coefficients of our formulation are avoided for all transitions $\nu_a \rightarrow \nu_b$ by transforming to a different set of coefficients presented in an appendix of this paper. The neutrino mass eigenvalues are easily obtained numerically as the solution of a cubic equation. Our methods are illustrated for flavor-changing transitions in the (ν_e, ν_μ) sector. The resulting analytic expressions oscillation probabilities, which are particularly simple, are also accurate to a few percent over all regions of interest at present and the envisioned future neutrino facilities. While somewhat less accurate than numerical simulations, our approximate expressions are sufficiently accuracy to obviate the need for exact computer simulations in many circumstances.

PACS Indices: 11.3.Er,14.60.Lm,13.15.+g

Keywords:

I. INTRODUCTION

In this paper, we develop methods leading to approximate analytical expressions for the oscillation probability from the exact, closed-form results in Ref. [1]. These results are based on a conventional Hamiltonian and the Standard Neutrino Model [2] and lead to expressions for the oscillation probability for all transitions $\nu_a \rightarrow \nu_b$.

We include the interaction of neutrinos with electrons shown to be essential by Wolfenstein in 1978 [3] and later identified by Mikheyev and Smirnov [4] as a likely explanation of the deficit of solar neutrinos discovered experimentally by Davis [5, 6].

Subsequent to the work of Wolfenstein, neutrino oscillations in matter have been commonly explored using exact computer simulations. These methods have advantages for density profiles having a spatial dependence, are discussed in Ref. [7] and references therein.

Comparisons of Ref. [1] to currently available analytical results [8–10] are found in Ref. [11], where it is established that these results [8–10] are reliable over rather narrow regions of energy, density, and baseline. Expressions found here do not suffer from these limitations.

In the present paper we use the published formulation of Ref. [1]. Because we rely heavily on all results found in Ref. [11], the reader will find many

of the important results of the unpublished Ref [11] repeated here.

Our formulation [1] is introduced in Sect. II with details relegated to appendices. The oscillation probability simplifies in part because many of the terms appearing in the exact coefficients $w_{i,p}^{(ab)}$ of our approach [1] are quite small [$O(\alpha^n)$, $n \geq 3$] and can therefore be eliminated.

The expressions we find for the oscillation probabilities are built on coefficients $w_{i,p^-}^{(ab)}$ that are devoid of subtle cancelations occurring in the coefficients $w_{i,p}^{(ab)}$ of Ref. [1]. The nature of these cancelations is discussed in Sect. III, and their source is identified in Sect. III B. The cancellations are avoided by making a transformation that leaves the partial oscillation probabilities invariant. The resulting coefficients $w_{i,p^-}^{(ab)}$ are essential for obtaining simple expressions for the observable oscillation probabilities accurate to $O(\alpha^2)$ [about 1%]. The coefficients $w_{i,p^-}^{(ab)}$ are tabulated in Appendix C of the present paper for all transitions $\nu_a \rightarrow \nu_b$.

Observable oscillation probabilities accurate to $O(\alpha^2)$ are easily found using $w_{i,p^-}^{(ab)}$ and eigenvalues obtained by numerically by solving a cubic equation. However, the emphasis of this paper is on developing methods for obtaining simple and accurate *analytical* expressions for the oscillation probabilities. These methods are based on the same coefficients $w_{i,p^-}^{(ab)}$.

Application of these methods is illustrated for flavor-changing transitions in the (ν_e, ν_μ) sector. The oscillation probabilities so obtained are accu-

rate to a few percent over all regions of interest at present and envisioned future neutrino facilities. While somewhat less accurate than numerical simulations, our approximate expressions are sufficiently accurate to obviate the need for exact computer simulations in many circumstances.

Our results rely on neutrino mass eigenvalues evaluated using first-order perturbation theory in one of the small parameters $\xi = (\alpha, \sin^2 \theta_{13})$ of the SNM. Within the solar resonance region, the simplest expressions accurate to $O(\alpha^2)$ are based on the $\sin^2 \theta_{13}$ -expanded eigenvalues. Above the solar resonance region they are based on the α -expanded eigenvalues.

The procedure for obtaining the *simplest* expressions for the oscillation probabilities for all transitions $\nu_a \leftrightarrow \nu_b$ is identified in Sect IV A 1. As before, we illustrate the procedure for the specific case of $\nu_e \rightarrow \nu_\mu$ transitions. Expressions for our simplified oscillation probabilities are given in Appendix VI.

As emphasized in Ref. [12], accurate and reliable expressions for oscillation probabilities are essential for analysis and prediction at future neutrino facilities. We calibrate these aspects of our results over all regions of energy and matter density of interest. In Sect. V, we present comparisons within the solar resonance region, and in Sect. VI we present comparisons above the solar resonance region.

II. NEUTRINO DYNAMICS

The dynamics of the three known neutrinos and their corresponding anti-neutrinos in matter is determined by the time-dependent Schroedinger equation,

$$i \frac{d}{dt} |\nu(t)\rangle = H_\nu |\nu(t)\rangle, \quad (1)$$

where the neutrino Hamiltonian H_ν ,

$$H_\nu = H_{0\nu} + H_1, \quad (2)$$

consists of a piece $H_{0\nu}$ describing neutrinos in the vacuum and a piece H_1 describing their interaction with matter.

Our formulation [1] applies to neutrinos propagating in a uniform medium for interactions constant not only in space but also time, and it assumes that that neutrinos and anti-neutrinos represented are the structureless elementary Dirac fields of the Standard Neutrino Model [2].

A. The Neutrino Hamiltonian in Matter

Neutrinos are characterized by flavor $f(\nu_e, \nu_\mu, \nu_\tau)$ and mass $m[\nu_1, \nu_2, \nu_3]$. These states are related by the neutrino analog of the familiar CKM matrix,

$$\nu_f = U \nu_m. \quad (3)$$

They are produced and detected in states of a specific flavor.

The unitary matrix U is often parametrized in terms of three mixing angles ($\theta_{12}, \theta_{13}, \theta_{23}$) and a phase δ_{cp} characterizing CP violation.

Using the standard abbreviations, $s_{12} \equiv \sin \theta_{12}$, $c_{12} \equiv \cos \theta_{12}$, etc,

$$U \equiv \begin{pmatrix} c_{12}c_{13} & s_{12}c_{13} & s_{13}e^{-i\delta_{cp}} \\ U_{21} & U_{22} & s_{23}c_{13} \\ U_{31} & U_{32} & c_{23}c_{13} \end{pmatrix}, \quad (4)$$

where,

$$\begin{aligned} U_{21} &= -s_{12}c_{23} - c_{12}s_{23}s_{13}e^{i\delta_{cp}} \\ U_{22} &= c_{12}c_{23} - s_{12}s_{23}s_{13}e^{i\delta_{cp}} \\ U_{31} &= s_{12}s_{23} - c_{12}c_{23}s_{13}e^{i\delta_{cp}} \\ U_{32} &= -c_{12}s_{23} - s_{12}c_{23}s_{13}e^{i\delta_{cp}}. \end{aligned} \quad (5)$$

In this representation, the index $i = 1$ of U_{ij} corresponds to the electron neutrino ν_e , the index $i = 2$ to the muon neutrino ν_μ , and the index $i = 3$ to the tau neutrino ν_τ .

The perturbing Hamiltonian H_1 is determined by the interaction between electron neutrino flavor states and the electrons of the medium. Expressed as matrix,

$$H_1 = U^{-1} \begin{pmatrix} V & 0 & 0 \\ 0 & 0 & 0 \\ 0 & 0 & 0 \end{pmatrix} U, \quad (6)$$

With $V = \pm\sqrt{2}G_F n_e$ and n_e the electron number density in matter.

B. The Standard Neutrino Model

For electrically neutral matter consisting of protons, neutrons, and electrons, the electron density n_e is the same as the proton density n_p ,

$$\begin{aligned} n_e &= n_p \\ &= RA, \end{aligned} \quad (7)$$

where $A = N + Z$ is the average total nucleon number density of matter through which the neutrinos propagate and $R = Z/A$ is its average proton-nucleon ratio. In the earth's mantle, the dominant constituents of matter are the light elements so $R \approx 1/2$; in the surface of a neutron star $R \ll 1$. Matrix elements of H_1 are thus

$$\langle M(k)|H_1|M(k') \rangle = U_{1k}^* V U_{1k'} . \quad (8)$$

Using the well-known expression for V , we find the corresponding the (dimensionless) interaction strength \hat{A} of neutrinos and anti-neutrinos with matter to be,

$$\hat{A} = \pm 6.50 \cdot 10^{-2} R E[\text{GeV}] \rho[\text{gm/cm}^3] , \quad (9)$$

with $E[\text{GeV}]$ being the neutrino beam energy in GeV and $\rho[\text{gm/cm}^3]$ the average total density of matter through which the neutrino beam passes on its way to the detector in gm/cm^3 . For experiments close to the earth's surface, the appropriate density is the mean density of the earth's mantle,

$$\begin{aligned} \rho[\text{gm/cm}^3] &= \rho_0 \\ &\approx 3 . \end{aligned} \quad (10)$$

We adopt the Standard Neutrino Model [2], given next, to complete our description of the neutrino Hamiltonian. Most of the parameters of the SNM are consistent with global fits to neutrino oscillation data with relatively good precision [13, 14]. These include the neutrino mass differences,

$$\begin{aligned} m_2^2 - m_1^2 &\equiv \delta m_{21}^2 \\ &= 7.6 \times 10^{-5} \text{ eV}^2 \end{aligned} \quad (11)$$

and

$$\begin{aligned} m_3^2 - m_1^2 &\equiv \delta m_{31}^2 \\ &= 2.4 \times 10^{-3} \text{ eV}^2 , \end{aligned} \quad (12)$$

which corresponds to

$$\begin{aligned} \alpha &\equiv \frac{\delta m_{21}^2}{\delta m_{31}^2} \\ &= 3.17 \times 10^{-2} . \end{aligned} \quad (13)$$

The mixing angles θ are also determined from experiment. In the SNM, the value of θ_{23} ,

$$\theta_{23} = \pi/4 , \quad (14)$$

is the best-fit value from Ref. [15], and θ_{12} ,

$$\theta_{12} = \pi/5.4 , \quad (15)$$

is consistent with the recent analysis of Ref. [16]. The mixing angle θ_{13} is known to be small ($\theta_{13} < 0.18$ at the 95% confidence level), but until recently its precise value has been quite uncertain. Results from the Daya Bay project [17] have measured its value more accurately, $\sin^2 \theta_{13} \approx 0.15$, which we adopt to determine our value for θ_{13} ,

$$\theta_{13} = 0.151 . \quad (16)$$

This fixes $R_p \equiv \sin^2 \theta_{13}/\alpha \approx 0.711$. The CP violating phase is not known at all, and determining its value will one of the major interests at future neutrino facilities.

C. Our Hamiltonian Formulation

Our approach is based on the evaluation of the time-evolution operator $S(t', t)$ using the Lagrange interpolation formula [18]. For time-independent interactions, $S(t', t)$ is written,

$$S(t', t) = e^{-iH_\nu(t'-t)} . \quad (17)$$

It depends on time only through the time *difference* $t' - t$ and mat then be written in terms of the stationary state solutions $|\nu_{mi} \rangle$ of Eq. (1),

$$S(t', t) = \sum_i |\nu_{mi} \rangle e^{-iE_i(t'-t)} \langle \nu_{mi} | . \quad (18)$$

Because the rest masses of neutrinos are considered to be tiny, for most cases of interest including our approach, the ultra-relativistic limit, $|\vec{p}| \gg m^2$ (we take the speed of light $c = 1$) is assumed. Ultra-relativistic neutrinos of energy E in the laboratory frame may be expressed,

$$E \approx |\vec{p}| + \frac{m^2}{2E} , \quad (19)$$

where m_i is its mass in the vacuum.

Thus, in this limit and in dimensionless variables,

$$\hat{E}_i \rightarrow \frac{M_i^2 - m_1^2}{m_3^2 - m_1^2} \quad (20)$$

and

$$\hat{H}_{0\nu} \rightarrow \begin{pmatrix} 0 & 0 & 0 \\ 0 & \alpha & 0 \\ 0 & 0 & 1 \end{pmatrix} \quad (21)$$

with

$$\alpha \equiv \frac{m_2^2 - m_1^2}{m_3^2 - m_1^2} . \quad (22)$$

The distance L from the source to the detector corresponding to $S(t', t)$ in Eq. (17) is

$$L = t' - t . \quad (23)$$

The time-evolution operator, Eq. (17), expressed in dimensionless variables is then,

$$\begin{aligned} S(L) &= e^{-iH_\nu(t'-t)} \\ &= e^{2i\hat{E}_1^0\Delta_L} e^{-2i\hat{H}_\nu\Delta_L} , \end{aligned} \quad (24)$$

where \hat{H}_ν is the full neutrino Hamiltonian expressed in dimensionless variables, and where

$$\Delta_L \equiv \frac{L(m_3^2 - m_1^2)}{4E} . \quad (25)$$

Our formulation is summarized in Appendix A.

Taking the value of δm_{21}^2 from the SNM, in the high-energy limit Δ_L [Eq. (25)] becomes,

$$\Delta_L \approx 3.05 \times 10^{-3} \frac{L[\text{Km}]}{E[\text{GeV}]} , \quad (26)$$

with $L[\text{Km}]$ the baseline in Km. From Eqs. (26,9), we find

$$\Delta_L \hat{A} = \pm 1.92 \cdot 10^{-4} R \rho[\text{gm/cm}^3] L[\text{Km}] , \quad (27)$$

or

$$L[\text{Km}] = \pm 5.05 \cdot 10^3 R \frac{\Delta_L \hat{A}}{\rho[\text{gm/cm}^3]} . \quad (28)$$

Neutrinos at rest in a neutron star were recently considered in Ref. [19]. It was recognized that the only modification required was to take the non-relativistic limit of the vacuum Hamiltonian. In our approach, this would mean taking

$$E_i^0 \rightarrow m_i + \frac{p^2}{2m_i} , \quad (29)$$

rather than Eq. (19). In particular, the eigenvalues of the interacting Hamiltonian continue to be expressed as the solution of the same cubic equation [see Eqs. (34,35) of Ref [1]] but now with $\alpha \rightarrow \hat{\alpha}$,

$$\hat{\alpha} \equiv \frac{m_2 - m_1}{m_3 - m_1} . \quad (30)$$

Because it is quite straightforward to obtain the eigenvalues by solving the cubic equation numerically, if all one requires is an answer, the preferable approach would be to obtain the oscillation probability in our Hamiltonian formulation using the expressions given in Appendix A with the coefficients given in Appendix C. The advantage of the analytical result we pursue in the remainder of the paper is the insight into the underlying physics that simple analytical results provide.

III. SMALL PARAMETER EXPANSIONS OF OBSERVABLE OSCILLATION PROBABILITIES

Our goal is to obtain the simplest possible expressions for the *observable* neutrino oscillation probabilities accurate to about 1%. This is accomplished using the small-parameter expansions of the exact analytical expressions of our formulation. The small-parameter expansion is facilitated by eliminating $\sin^2 \theta_{13}$ in favor of α , writing $\sin^2 \theta_{13} = R_p \alpha$, and then expanding in α . Because $R_p \approx 0.711$ in the SNM, a Taylor expansion in α avoids having to expand separately in α and $\sin^2 \theta_{13}$ to simplify expressions.

A. The Observable Oscillation Probabilities

The observable oscillation probabilities are expressed in terms of the partial oscillation probabilities defined in Ref. [1] and summarized in Appendix A of this paper. Our methods are applicable to these oscillation probabilities for all transitions $\nu_a \rightarrow \nu_b$.

One of the observable oscillation probabilities, $P^{+ab}(\Delta_L, \hat{A})$, is the sum over three of the four partial oscillation probabilities defined in Eq. (A2) and is symmetric under $a \leftrightarrow b$,

$$\begin{aligned} P^{+ab}(\Delta_L, \hat{A}) &\equiv P_{\cos\delta}^{ab}(\Delta_L, \hat{A}) + P_{\cos^2\delta}^{ab}(\Delta_L, \hat{A}) \\ &\quad + P_0^{ab}(\Delta_L, \hat{A}) . \end{aligned} \quad (31)$$

The structure of $P^{+ab}(\Delta_L, \hat{A})$ is rather complicated, and simplifying this quantity is the focus of this paper.

The other observable oscillation probability, $P_{\sin\delta}^{ab}(\Delta_L, \hat{A})$, is defined in Eq. (A1). It is antisymmetric under $a \leftrightarrow b$. Because $P_{\sin\delta}^{ab}(\Delta_L, \hat{A})$ is both exact and already sufficiently simple, it will not be discussed further in this paper.

B. Leading Terms of the α -Expanded $w_{i,p}^{(ab)}$

A key quantity of our formulation [1] is the set of coefficients $w_{i,p}^{(ab)}$ given explicitly in Ref. [11]. These coefficients are polynomials in α , and for the purpose of the present work, it is rather important to note that for many transitions $\nu_a \rightarrow \nu_b$, the terms in the polynomial expressions for $w_{i,p}^{(ab)}$ with the lowest powers in α (the ‘‘leading terms’’) cancel against

each other when $\hat{E}_\ell \approx 1$ or $\hat{E}_\ell \approx 0$. One or both of these conditions hold for at least one or two of the eigenvalues over nearly the entire range of \hat{A} . The consequence is that if we express the oscillation probabilities in terms of the original set of coefficients $w_{i;p}^{(ab)}$, three powers of α must be retained to achieve $O(\alpha^2)$ accuracy, whereas we might have expected to retain only two. Polynomials with two powers of α are, of course, simpler than those with three.

Polynomials with $O(\alpha^2)$ accuracy with two powers of α do, in fact, exist. To find them, it is important to recognize that there is nothing unique about the original set of coefficients $w_{i;p}^{(ab)}$. We could have chosen any set of coefficients say, $w_{i;p^-}^{(ab)}$, as long as the partial oscillation probabilities remain invariant under $w_{i;p}^{(ab)} \rightarrow w_{i;p^-}^{(ab)}$. An example of such a transformation is,

$$\begin{aligned} w_{i;0^-}^{(ab)} &\equiv w_{i;0}^{(ab)} + w_{i;1}^{(ab)} + w_{i;2}^{(ab)} \\ w_{i;1^-}^{(12)} &\equiv w_{i;1}^{(12)} + w_{i;2}^{(12)} \\ w_{i;2^-}^{(12)} &\equiv w_{i;2}^{(12)}. \end{aligned} \quad (32)$$

Clearly, the partial oscillation probabilities are invariant under this transformation since,

$$\begin{aligned} \hat{w}_i^{ab}[\ell] &\rightarrow (w_{i;0^-}^{(ab)} + w_{i;1^-}^{(ab)}(\hat{E}_\ell - 1) + w_{i;2^-}^{(ab)} \\ &\quad \times \hat{E}_\ell(\hat{E}_\ell - 1))\Delta\hat{E}[\ell] \\ &= (w_{i;0}^{(ab)} + w_{i;1}^{(ab)}\hat{E}_\ell + w_{i;2}^{(ab)}\hat{E}_\ell^2) \\ &\quad \times \Delta\hat{E}[\ell]. \end{aligned} \quad (33)$$

The important points to note are, first, that the terms in the polynomial expressions for $w_{i;p^-}^{(ab)}$, $p = 0, 1, 2$ having the lowest powers in α cancel only in isolated cases. Secondly, the quantity $\hat{w}_i^{ab}[\ell]$ is expressed equivalently in terms of both $w_{i;p^-}^{(ab)}$ and $w_{i;p}^{(ab)}$. Thus, the simplest expressions for the oscillation probabilities of $O(\alpha^2)$ accuracy are found from the first two powers in α in the expansion of $w_{i;p^-}^{(ab)}$, whereas the same accuracy using $w_{i;p}^{(ab)}$ would require the first three powers of α . The coefficients $w_{i;p^-}^{(ab)}$ and $w_{i;p}^{(ab)}$ are, of course, no longer equivalent when they are truncated.

Next, we compare calculations of an approximate oscillation probability using the first two leading terms of $w_{i;p^-}^{(e\mu)}$ with an exact oscillation probability calculated with $w_i^{ab}[\ell]$.

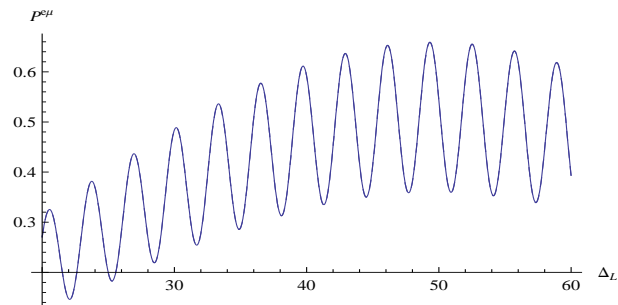


FIG. 1. Neutrino total oscillation probability $P^{e\mu}(\Delta_L, \hat{A})$ as a function of Δ_L for $\hat{A} = 0.102$. Exact result (solid curve); approximate result (dashed curve) calculated using exact eigenvalues and the first two leading terms of $w_{i;p^-}^{(e\mu)}$. All parameters except δ_{cp} are determined by the SNM.

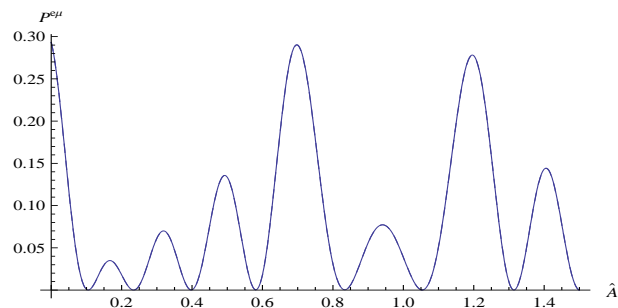


FIG. 2. Neutrino total oscillation probability $P^{e\mu}(\Delta_L, \hat{A})$ as a function of \hat{A} for $\Delta_L = 20$ and $\delta_{cp} = \pi/4$. Full theory (solid curve); approximate result (dashed curve) calculated using exact eigenvalues and the first two leading terms of $w_{i;p^-}^{(e\mu)}$. All parameters except δ_{cp} are determined by the SNM.

Figure 1 shows a comparison of the two calculations of $P^{e\mu}(\Delta_L, \hat{A})$ over the interval $20 < \Delta_L < 60$ for a value of $\hat{A} = 0.102$. In Fig. 2 shows a comparison of the two calculations of $P^{e\mu}(\Delta_L, \hat{A})$ over the interval $0 < \hat{A} < 1.5$ for fixed $\Delta_L = 20$. As expected, the calculation using the first two leading terms of $w_{i;p^-}^{(e\mu)}$ agrees very well with the exact one in both cases.

We have examined the percentage error in the partial oscillation probabilities $P_{cos}^{e\mu}(\Delta_L, \hat{A})$ and $P_0^{e\mu}(\Delta_L, \hat{A})$ calculated using the first two leading terms of $w_{i;p^-}^{(e\mu)}$ by comparing them numerically to the exact result. The exact and approximate calculations agree within a fraction of a percent, except in the vicinity of zeros. The error unavoidably diverges sufficiently close to the zeros when they are

displaced by even a small amount.

We find the same cancellation just discussed for $\nu_e \rightarrow \nu_\mu$ transitions occurs for most of the other transitions as well. We have tabulated the truncated coefficients $w_{i,p^-}^{(ab)}$ for all these transitions in Appendix C.

The coefficients $w_{i,p^-}^{(ab)}$, used in conjunction with a numerical evaluation of the neutrino mass eigenvalues, make it possible to find simple expressions for the observable oscillation probabilities applicable to all transitions $\nu_a \rightarrow \nu_b$ accurate to $O(\alpha^2)$ [about 1%] throughout the entire region of interest at present and envisioned future neutrino facilities. The mass eigenvalues are easily obtained numerically as the solution of a cubic equation.

IV. SIMPLE ANALYTIC EXPRESSIONS FOR $P^{+ab}(\Delta_L, \hat{A})$

In this section, we develop methods that lead to simple analytic expressions for the observable oscillation probabilities of all transitions $\nu_a \rightarrow \nu_b$. The analytical results are simple, in part, because many of the terms appearing in the exact coefficients of our approach [1] are quite small [$O(\alpha^n)$, $n \geq 3$] and, for this reason, can be eliminated. Application of the methods is illustrated for flavor-changing transitions in the (ν_e, ν_μ) sector.

A. Simplifying $P^{+ab}(\Delta_L, \hat{A})$

Consider the partial oscillation probability $P_i^{ab}(\Delta_L, \hat{A})$ contributing to $P^{+ab}(\Delta_L, \hat{A})$ in Eq. (31). The idea making it possible to find remarkably simple expressions for $P^{+ab}(\Delta_L, \hat{A})$ can be explained in terms of the $\hat{w}_i^{ab}[\ell]$ corresponding to $P_i^{ab}(\Delta_L, \hat{A})$ as follows.

Expanding $\hat{w}_i^{ab}[\ell]$ we find

$$\hat{w}_i^{ab}[\ell] = \sum_{n,i} C_{n,i}(\ell, \alpha) \hat{A}^n, \quad (34)$$

where, of course,

$$\begin{aligned} \hat{w}_i^{ab}[\ell] &\equiv (w_{i;0}^{(ab)} + w_{i;1}^{(ab)}) \hat{E}_\ell + w_{i;2}^{(ab)} \hat{E}_\ell^2 \\ &\times \Delta \hat{E}[\ell], \end{aligned} \quad (35)$$

and $C_{n,i}(\ell, \alpha)$ is the coefficient of \hat{A}^n in the expansion of $\hat{w}_i^{ab}[\ell]$. Then, expanding $C_{n,i}(\ell, \alpha)$ and re-

taining the first two terms in the power series in α ,

$$\begin{aligned} C_{n,i}(\ell, \alpha) &\approx \alpha^p(n) (C(\ell)_{0;n,i} \\ &+ \alpha C(\ell)_{1;n,i} + \dots). \end{aligned} \quad (36)$$

From these expressions, we can easily see that evaluating $P^{+ab}(\Delta_L, \hat{A})$ in terms of individual $P_i^{ab}(\Delta_L, \hat{A})$ accurate to about 1% fails to give the simplest expressions for $P^{+ab}(\Delta_L, \hat{A})$ when $\hat{w}_0^{e\mu}[\ell] \gg \hat{w}_{\cos}^{e\mu}[\ell]$ or $\hat{w}_{\cos}^{e\mu}[\ell] \gg \hat{w}_0^{e\mu}[\ell]$. Said otherwise, when $\hat{w}_0^{e\mu}[\ell] \gg \hat{w}_{\cos}^{e\mu}[\ell]$ or $\hat{w}_{\cos}^{e\mu}[\ell] \gg \hat{w}_0^{e\mu}[\ell]$, simplifying the individual $P_i^{ab}(\Delta_L, \hat{A})$ before simplifying $P^{+ab}(\Delta_L, \hat{A})$ does not lead to the simplest expression for $P^{+ab}(\Delta_L, \hat{A})$.

In this situation, the approach that does work is to first “consolidate” the coefficients $\hat{w}_i^{ab}[\ell]$, which means to (1) construct the single quantities $\hat{w}_i^{ab}[\ell]$ defined in Eq. (38); (2) simplify $\hat{w}_i^{ab}[\ell]$; and, (3) construct $P^{+ab}(\Delta_L, \hat{A})$ from this simplified $\hat{w}_i^{ab}[\ell]$. The reason why consolidation works is most easily understood by considering $C(\Delta_L, \hat{A})$,

$$\begin{aligned} C(\Delta_L, \hat{A}) &\equiv -\frac{4\Delta_L^2}{\hat{D}} \sum_{\ell} (-1)^{\ell} \hat{w}^{ab}[\ell] \\ &\times j_0^2(\Delta_L \hat{E}[\ell]), \end{aligned} \quad (37)$$

where,

$$\begin{aligned} \hat{w}^{ab}[\ell] &\equiv \cos \delta_{cp} \hat{w}_{\cos}^{(ab)}[\ell] + \cos^2 \delta_{cp} \hat{w}_{\cos^2}^{(ab)}[\ell] \\ &+ \hat{w}_0^{(ab)}[\ell]. \end{aligned} \quad (38)$$

The quantity $C(\Delta_L, \hat{A})$ bears a simple relation to $P^{+ab}(\Delta_L, \hat{A})$,

$$P^{+ab}(\Delta_L, \hat{A}) = C(\Delta_L, \hat{A}). \quad (39)$$

The important point is that when $\hat{w}_0^{e\mu}[\ell] \gg \hat{w}_{\cos}^{e\mu}[\ell]$ or $\hat{w}_{\cos}^{e\mu}[\ell] \gg \hat{w}_0^{e\mu}[\ell]$, the smaller coefficients are seldom among the first two leading terms of $\hat{w}^{ab}[\ell]$ defined in Eq. (38) and, for this reason, they do not appear in the simplified $C(\Delta_L, \hat{A})$. However, when the individual $\hat{w}_i^{ab}[\ell]$ of Eq. (35) are simplified, these small terms are often retained and appear in $P^{+ab}(\Delta_L, \hat{A})$ when they are added together to obtain $P^{+ab}(\Delta_L, \hat{A})$.

The quantity \hat{D} appearing in Eq. (37) is different for each region. In particular, $\hat{D} = \alpha C_T (1 - \alpha(1 + R_s))$ within the deep solar resonance region, $\hat{D} = \alpha C_T (R_s - \alpha(1 + R_s))/R_s^2$ within the far solar resonance region, and $\hat{D} = \hat{C}_\alpha (\hat{A} - \alpha(c_{12} + \hat{A}(c_{12} + R_p)))$ above the solar resonance region.

In Eq. (38), the quantity $\hat{w}_i^{(ab)}[\ell]$ is,

$$\begin{aligned} \hat{w}_i^{(ab)}[\ell] &= (w_{i;0^-}^{(ab)} + w_{i;1^-}^{(ab)}(\hat{E}_\ell - 1) + w_{i;2^-}^{(ab)}) \\ &\quad \times \hat{E}_\ell(\hat{E}_\ell - 1)\Delta\hat{E}[\ell], \end{aligned} \quad (40)$$

where the coefficients $w_{i;p^-}^{(ab)}$ are found in Appendix C for all transitions $\nu_a \rightarrow \nu_b$.

1. $\hat{C}_\alpha(\hat{A})$ and $C_T(R_s)$: Independent Variables

The error in $P^{+ab}(\Delta_L, \hat{A})$, so consolidated, is most easily seen to be of order of 1% by dropping all terms of relative size α^n with $n > 1$ and recognizing that $\alpha \approx 0.0317$ [see Eq. (13)]. Said otherwise, an accuracy of about 1% is achieved by retaining just the first two terms of the α -expansion of $C_{n,i}(\ell, \alpha)$ ($C(\ell)_{0;n,i}$ and $C(\ell)_{1;n,i}$).

In this case, $P_i^{ab}(\Delta_L, \hat{A})$ takes the form,

$$\begin{aligned} P_i^{ab}(\Delta_L, \hat{A}) &\rightarrow -\frac{4\Delta_L^2}{\hat{D}} \sum_{n,\ell} \alpha^p(n)(C(\ell)_{0;n,i} + \alpha C(\ell)_{1;n,i}) \\ &\quad \times \hat{A}^n j_0^2(\Delta_L \Delta\hat{E}[\ell]). \end{aligned} \quad (41)$$

Equation 41) is valid only when \hat{C}_α is taken to be independent of \hat{A} , but the argument is easily generalized to take account of the dependence of \hat{C}_α on \hat{A} (see Sect. IV A 2). Similar ideas apply to expressions within the solar resonance region where $\hat{C}_\alpha \rightarrow C_T$.

2. $\hat{C}_\alpha(\hat{A})$ and $C_T(R_s)$: Dependent Variables

Of course, \hat{C}_α and C_T are actually independent variables. We next consider the more realistic case where \hat{C}_α depends on \hat{A} and C_T depends on R_s .

Although this discussion is somewhat technical, it explains in detail how we found the simplified expressions for $P_i^{+e\mu}(\Delta_L, \hat{A})$ given in Appendix IV, on which the numerical results of Sects. V and VI documenting their accuracy is based. Because this discussion is general, it applies to all transitions $\nu_a \rightarrow \nu_b$. Although we assume that we are above the solar resonance region, the argument applies equally as well within the solar resonance region by replacing $\hat{C}_\alpha \rightarrow C_T$.

When $\hat{C}_\alpha \rightarrow \hat{C}_\alpha(\hat{A})$, we first factor $C(\Delta_L, \hat{A})$, Eq. (37). One of these factors is proportional to $1/C_\alpha^3(\hat{A})$. This dependence arises from the ξ -expanded eigenvalues appearing in Appendix B of Ref [11] and associated with the term $w_{i;2^-}^{(ab)} \hat{E}_\ell^2 \Delta\hat{E}[\ell]$. The product of the other factors is proportional to $C_\alpha^m(\hat{A})$, $m = 0, 1, 3, 5, \dots$

We then replace each term proportional to an even power, say $2n$, of $\hat{C}_\alpha(\hat{A})$ by $\hat{C}_\alpha(\hat{A})^{2n} \rightarrow ((1 - \hat{A})^2 + 4\alpha R_p \hat{A})^n$. Similarly, each term proportional to an odd power, say $2n + 1$, of $\hat{C}_\alpha(\hat{A})$ by $\hat{C}_\alpha(\hat{A})^{2n+1} \rightarrow ((1 - \hat{A})^2 + 4\alpha R_p \hat{A})^n \hat{C}_\alpha(\hat{A})$.

After these replacements, a straightforward generalization of Eq. (41) gives,

$$C(\Delta_L, \hat{A}) \rightarrow -\frac{4\Delta_L^2}{\hat{D}C_\alpha^3} \sum_{n,\ell} \alpha^p(n)((C(\ell)_{0;n} + \alpha C(\ell)_{1;n}) + \hat{C}_\alpha(C'(\ell)_{0;n} + \alpha C'(\ell)_{1;n}))\hat{A}^n j_0^2(\Delta_L \Delta\hat{E}[\ell]), \quad (42)$$

where $C(\ell)_{0;n}$, $C(\ell)_{1;n}$ and $C'(\ell)_{0;n}$, $C'(\ell)_{1;n}$ are the two sets of first two leading terms of $\hat{w}^{ab}[\ell]$.

3. Summary and Discussion

To summarize, by expressing $P^{+ab}(\Delta_L, \hat{A})$ in terms of the single coefficient $\hat{w}^{ab}[\ell]$ in Eq. (40), the entire set of terms $\hat{w}_0^{e\mu}[\ell]$ and $\hat{w}_{cos}^{e\mu}[\ell]$ are collected together with the consequence that the first two leading terms of $P^{+ab}(\Delta_L, \hat{A})$ is $O(\alpha^2)$.

At the same time, some of the higher-order terms that would have been retained by considering $\hat{w}_0^{e\mu}[\ell]$

and $\hat{w}_{cos}^{e\mu}[\ell]$ independently are naturally discarded, leading to the *simplest* result of $O(\alpha^2)$. It is the *simplest* result of $O(\alpha^2)$ because the combination has fewer terms when one of the two $\hat{w}_i^{e\mu}[\ell]$ is smaller than the other. Inspection of the coefficients given in Appendix D indicates that this is often the case.

Since the first two leading terms constitute the simplest and most accurate expressions for the oscillation probability, this method is guaranteed to lead uniquely to the simplest and most accurate expression for $P^{+ab}(\Delta_L, \hat{A})$ to about 1%, which is what we set out to find. We note in passing that we have managed to cast ‘‘simplicity’’ into mathematical language. Some might find this interesting, since ‘‘sim-

plicity is normally considered to be a subjective concept.

The resulting oscillation probabilities were seen to be accurate to a few percent over all regions of interest at present and envisioned future neutrino facilities. These analytic oscillation probabilities are vastly more accurate than the familiar analytic expressions on the interval $0 < \hat{A} < \alpha$ and for values of \hat{A} extending from 0.35 well into the asymptotic region, $\hat{A} \gg 1$. While somewhat less accurate than numerical simulations, our approximate expressions are sufficiently accurate to obviate the need for exact computer simulations in many circumstances. The accuracy of the approximate $P^{+ab}(\Delta_L, \hat{A})$ found in this way is sufficient for analysis and prediction of experiments at present and future neutrino facilities. Furthermore, the accuracy is easy improved applying a well-defined correction procedure.

Note the following caveats. Depending on the values of the parameters of the SNM, for specific regions it may happen that (1) some pieces of the first two leading terms are small enough to drop to maintain a specific accuracy goal; (2) the terms of relative order α^2 may happen to be anomaly large and thus retained to maintain an accuracy goal.

These results may be used to define “effective” partial oscillation probabilities. The “effective” partial oscillation probability $P_{\cos\delta}^{ab}(\Delta_L, \hat{A})$ would represent the dependence of $P^{+ab}(\Delta_L, \hat{A})$ on δ_{cp} . Similarly, an “effective” partial oscillation probability $P_{\cos^2\delta}^{ab}(\Delta_L, \hat{A})$ would represent the dependence of $P^{+ab}(\Delta_L, \hat{A})$ on δ_{cp}^2 , and an “effective” $P_0^{ab}(\Delta_L, \hat{A})$ would represent terms independent of δ_{cp} . These effective partial oscillation determine, in turn, effective $\hat{w}_i^{e\mu}[\ell]$. Note, however, that these effective partial oscillation probabilities are not guaranteed to be the simplest to $O(\alpha^2)$.

V. SIMPLIFIED PARTIAL OSCILLATION PROBABILITIES, $\hat{A} < 0.1$

In this section, we consider the simplified oscillation probability over the interval $0 < \hat{A} < \hat{A}_f$, where, in this paper, $\hat{A}_f = 0.1$. This interval encompasses the solar resonance, which is located at $\hat{A} = \alpha$. For this reason, the interval $0 < \hat{A} < 0.1$ is referred to in this paper as the solar resonance region. Note that this definition of the solar resonance region differs from that adopted in Ref. [1], where $\hat{A}_f = 0.2$.

Here, we split up the solar resonance region into

two sub-regions. The sub-region $0 < \hat{A} < \alpha$ is referred to as the deep solar region, and the sub-region $\alpha < \hat{A} < 0.1$ as the far solar region. For these sub-regions, we find it sufficient to retain only the first leading term of eigenvalue difference, *i.e.*, $\Delta\hat{E}[\ell] = \Delta\hat{E}_0[\ell]$, where $\Delta\hat{E}_0[\ell]$ is the first term of the Taylor series expansion of $\Delta\hat{E}[\ell]$ in $\sin^2\theta_{13}$ appearing in Appendix IV B.

The simplified $P^{+ab}(\Delta_L, \hat{A})$ within the solar resonance region is given explicitly in Appendix VI by applying the procedure of Sect. IV. We examine this $P^{+ab}(\Delta_L, \hat{A})$ numerically in the present section. By comparing $P^{+ab}(\Delta_L, \hat{A})$ to its exact counterpart, we will establish that $P^{+ab}(\Delta_L, \hat{A})$ describes the \hat{A} - and Δ_L -dependence of the exact oscillation probability within the solar resonance region much more reliably than those presently found in the literature.

A. General Considerations

From the simplified expressions for $P^{+ab}(\Delta_L, \hat{A})$ given in Appendix VI, where our results are expressed in terms of effective partial oscillation probabilities and effective $\hat{w}_i^{e\mu}[\ell]$, we will see that the effective $\hat{w}_{\cos\delta}^{e\mu}[\ell]$ is generally non-vanishing. For this reason, $P^{+ab}(\Delta_L, \hat{A})$ is sensitive to the CP violating phase, δ_{cp} throughout this region. We will also see there that the situation is different above the solar resonance region.

Within the solar resonance region, the expansion in $\sin^2\theta_{13}$ is the appropriate one to use to obtain the eigenvalues. We use the representation of the $\sin^2\theta_{13}$ -expanded eigenvalues given in Appendix of Ref. [11]. This representation motivates splitting the solar resonance region into the deep solar resonance region, $\hat{A} < \alpha$ and the far solar resonance region, $\hat{A} > \alpha$.

The advantage of this representation is that by making the replacement,

$$\begin{aligned} \hat{A} &\rightarrow \alpha R_s \\ \hat{C}_\theta(\hat{A}) &\rightarrow \alpha C_T(R_s), \end{aligned} \quad (43)$$

in the eigenvalues of the deep solar resonance region, and,

$$\begin{aligned} \hat{A} &\rightarrow R_s/\alpha \\ \hat{C}_\theta(\hat{A}) &\rightarrow \hat{A} C_T(R_s), \end{aligned} \quad (44)$$

in those of the far solar resonance region, the *same* function of R_s ,

$$C_T(R_s) \equiv \sqrt{1 + R_s^2 - 2R_s \cos 2\theta_{12}}, \quad (45)$$

appears in both sets of eigenvalues.

Expressions for the effective partial oscillation probabilities given in Appendix VI have been simplified using the properties that for all $\hat{A} > 0$, R_s is positive and less than or equal to one and that

$$C_T(R_s) = 1 + O(\alpha) . \quad (46)$$

These properties have definite advantages for simplifying the analytic expressions we present below. In these expressions, we sometimes use C_T as an abbreviation for $C_T(R_s)$.

1. The Bessel functions $j_0^2(\Delta_L \Delta \hat{E}[\ell])$ and \hat{D}

Within the solar resonance region, we find it sufficient to evaluate the Bessel functions and \hat{D} in terms of the first term of the Taylor series expansion of the eigenvalue difference $\Delta \hat{E}[\ell]$. The first term $\Delta \hat{E}_0[\ell]$ is given in Appendix IV B.

Accordingly, the Bessel functions are expressed as,

$$j_0^2(\Delta_L \Delta \hat{E}[\ell]) = \frac{\sin^2 \Delta_L \Delta \hat{E}_0[\ell]}{\Delta \hat{E}_0^2[\ell]} , \quad (47)$$

within the deep solar resonance region. The energy denominator \hat{D} is expressed as,

$$\hat{D} = \alpha C_T (1 - \alpha(1 + R_s)) , \quad (48)$$

within the deep solar resonance region and,

$$\hat{D} = \frac{\alpha C_T}{R_s^2} (R_s - \alpha(1 + R_s)) , \quad (49)$$

within the far solar resonance region.

Within the solar resonance region, the oscillation probability $P^{+e\mu}(\Delta_L, \hat{A})$ is

$$\begin{aligned} P^{+e\mu}(\Delta_L, \hat{A}) &\rightarrow -\frac{4}{\hat{D}} \sum_{i,\ell} (-1)^\ell \hat{w}_i^{e\mu}[\ell] \\ &\times \frac{\sin^2 \Delta_L \Delta \hat{E}_0[\ell]}{\Delta \hat{E}_0^2[\ell]} . \end{aligned} \quad (50)$$

Numerical results for the oscillation probability $P^{+e\mu}(\Delta_L, \hat{A})$ calculated within deep the solar resonance region is give below in Sects. V B 1 and within the far solar resonance region in Sect V C.

B. Oscillation Probability $P^{+e\mu}(\Delta_L, \hat{A})$ within the Deep Solar Resonance Region

Within the deep solar resonance region, the relationship between the variables \hat{A} and R_s is $\hat{A} = \alpha R_s$. The energy denominator \hat{D} in this region is given in Eq. (48). The effective $\hat{w}_i^{e\mu}[\ell]$, in addition to the eigenvalue differences from which the Bessel functions and energy denominator are calculated, are given in Table II of Appendix VI.

1. Numerical Results in the Deep Solar Resonance Region

Figures 3 and 4 show $P^{+e\mu}(\Delta_L, \hat{A})$ compared to the exact oscillation probability as a function of \hat{A} and Δ_L , respectively. We see from these figures that $P^{+e\mu}(\Delta_L, \hat{A})$ and the exact oscillation probability agree to a high level of accuracy within the deep solar resonance region.

The other point of interest here is the extent to which $P^{+e\mu}(\Delta_L, \hat{A})$ is an improvement over the familiar approximate formulations. This may be assessed by comparing the \hat{A} and Δ_L dependences of the present theory and the full oscillation probability of AHLO.

This assessment of their \hat{A} dependence follows from a comparison of Fig. 3 to Fig. 3 of Ref. [11], which shows the AHLO and exact oscillation probabilities as a function of \hat{A} . We see from Fig. 3 of Ref. [11] that the full oscillation probability of AHLO overestimates the exact oscillation probability by about a factor of two over the interval $0 < \hat{A} < \alpha$, indicating that our simplified $P^{+e\mu}(\Delta_L, \hat{A})$ is a significant improvement over that of AHLO over this interval.

An assessment of the Δ_L dependence requires a comparison of the Δ_L dependence of the AHLO and exact oscillation probabilities. We have made such a comparison within the deep solar resonance region for $\hat{A} \approx \alpha/3$, finding hat the AHLO result agrees with the exact result comparatively well out to $\Delta_L \approx 30$, where they begin to diverge. The divergence continues to grow as Δ_L increases.

We see from this result and Fig. 3 that our simplified $P^{+e\mu}(\Delta_L, \hat{A})$ agrees quite well with AHLO for small values of Δ_L but not for the larger values, where all three Bessel functions interfere.

We thus find that $P^{+e\mu}(\Delta_L, \hat{A})$ is more accurate than the full expression of AHLO by examining the \hat{A} and the Δ_L dependence of the oscillation probability. We conclude that $P^{+e\mu}(\Delta_L, \hat{A})$ is a significant

improvement over the full expression of AHLO.

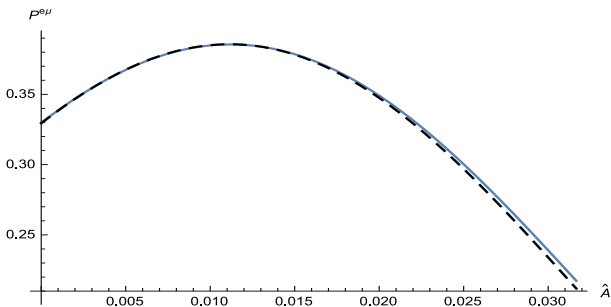


FIG. 3. $P^{+e\mu}(\Delta_L, \hat{A})$ for $\Delta_L = 60$ over the interval $0 < \hat{A} < \alpha$ for neutrinos in matter. All parameters except δ_{cp} are determined by the SNM. Exact result (solid curve); simplified result within deep solar resonance region calculated as described above (medium-dashed curve).

C. Oscillation Probability within the Far Solar Resonance Region

Within the far solar resonance region, the relationship between the variables \hat{A} and R_s is $\hat{A} = \alpha/R_s$. The energy denominator in this region is \hat{D} given in Eq. (49). The effective $\hat{w}_i^{e\mu}[\ell]$, in addition to the eigenvalue differences from which the Bessel functions and energy denominator are calculated are calculated are given in Table III of Appendix VI.

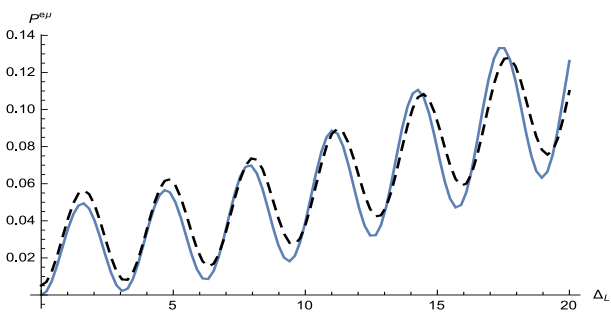


FIG. 4. $P^{+e\mu}(\Delta_L, \hat{A})$ for $\hat{A} = \alpha/2$ over the interval $0 < \Delta_L < 60$ for neutrinos in matter. All parameters except δ_{cp} are determined by the SNM. Exact result (solid curve); simplified result within deep solar resonance region calculated as described above (medium-dashed curve).

1. Numerical Results in the Far Solar Resonance Region

Figures 5 and 6 show $P^{+e\mu}(\Delta_L, \hat{A})$ compared to the exact oscillation probability as a function of \hat{A} and Δ_L , respectively. We see from these figures that $P^{+e\mu}(\Delta_L, \hat{A})$ and the exact oscillation probability agree to a high level of accuracy within the far solar resonance region.

As before, the other point of interest is again the extent to which $P^{+e\mu}(\Delta_L, \hat{A})$ is an improvement over the familiar approximate formulations. This may be assessed by comparing the \hat{A} and Δ_L dependences of the present theory and the full oscillation probability of AHLO.

This assessment of their \hat{A} dependence follows from a comparison of Fig. 5 to Fig. 4 of Ref. [11], which shows the AHLO and exact oscillation probabilities as a function of \hat{A} . Comparing Fig. 5 to Fig. 4 of Ref. [11], one sees that the full result of AHLO does reasonably well for $\alpha < \hat{A} < 0.1$, but our simplified result [medium-dashed curve in Fig. 5] does even better. This indicates that whereas our simplified $P^{+e\mu}(\Delta_L, \hat{A})$ might have some advantage over AHLO, this advantage is marginal.

An assessment of the Δ_L dependence requires a comparison of the Δ_L dependence of the AHLO and exact oscillation probabilities. We have made such a comparison within the far solar resonance region for $\hat{A} \approx 0.05$ over the interval $5 < \Delta_L < 55$ and finding that the AHLO result agrees with the exact result comparatively well over this interval, even for the larger values, where all three Bessel functions interfere.

Although our simplified $P^{+e\mu}(\Delta_L, \hat{A})$ is just marginally more accurate than the full expression of AHLO the full result of Ref. [9] is exceedingly complex [11]. Thus, within the far solar resonance region, our simplified $P^{+e\mu}(\Delta_L, \hat{A})$ is preferable to the full result of Ref. [9] because it is much simpler and more easily calculated than the full result of AHLO.

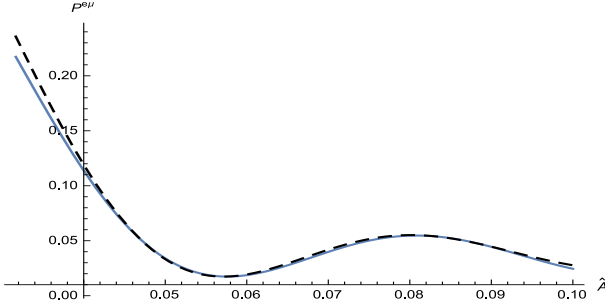


FIG. 5. $P^{+e\mu}(\Delta_L, \hat{A})$ for $\Delta_L = 60$ over the interval $\alpha < \hat{A} < 0.1$ for neutrinos in matter. All parameters except δ_{cp} are determined by the SNM. Exact result (solid curve); simplified result within Far solar resonance region calculated as described above (medium-dashed curve).

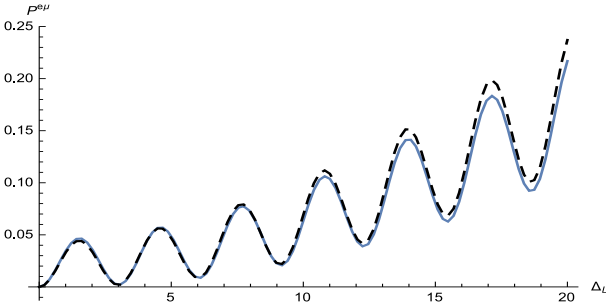


FIG. 6. $P^{+e\mu}(\Delta_L, \hat{A})$ for $\hat{A} = \alpha/2$ over the interval $0 < \Delta_L < 20$ for neutrinos in matter. All parameters except δ_{cp} are determined by the SNM. Exact result (solid curve); simplified result within far solar resonance region calculated as described above (medium-dashed curve).

VI. SIMPLIFIED OSCILLATION PROBABILITIES, $\hat{A} > 0.1$

In this section, we consider the simplified $P^{+ab}(\Delta_L, \hat{A})$ for values of \hat{A} above the solar resonance region. As defined in this paper, the solar resonance region encompasses the interval $0 < \hat{A} < \hat{A}_f$, where $\hat{A}_f = 0.1$. Note that this definition of the solar resonance region differs from that defined in Refs. [1, 11], where $\hat{A}_f = 0.2$.

We split up the interval $\hat{A} > 0.1$ into four sub-regions. The sub-region $0.1 < \hat{A} < 0.35$ is referred to as the lower transition region, and $0.35 < \hat{A} < \hat{A}_2$ as the upper transition region. The upper and lower transition sub-regions together constitute the transition region as defined in Refs. [1, 11]. The sub-region $\hat{A}_2 < \hat{A} < 1.2$ is referred to as the atmo-

spheric resonance region, and the sub-region $\hat{A} > 1.2$ as the asymptotic region. The atmospheric resonance and asymptotic sub-regions are both defined here as in Refs. [1, 11]. For these sub-regions, we find it necessary to retain both the first and the second leading terms of the eigenvalue differences, *i.e.*, $\Delta\hat{E}[\ell] = \Delta\hat{E}_0[\ell](1+r[\ell])$, where $\Delta\hat{E}_0[\ell]$ and $r[\ell]$ are given in Appendix IV C.

The simplified $P^{+ab}(\Delta_L, \hat{A})$ is given explicitly in Appendix VI by applying the procedure of Sect. IV. We examine this $P^{+ab}(\Delta_L, \hat{A})$ numerically in the present section. By comparing $P^{+ab}(\Delta_L, \hat{A})$ to its exact counterpart, we will establish that $P^{+ab}(\Delta_L, \hat{A})$ describes the \hat{A} - and Δ_L -dependence of the exact oscillation probability within the solar resonance region much more reliably than those presently found in the literature.

A. General Considerations

We find that in all sub-regions except for the lower transition sub-region, the effective $P_{cos}^{+e\mu}(\Delta_L, \hat{A})$ vanishes. Consequently, the entire sensitivity to the CP-violating phase δ_{cp} for these values of \hat{A} arises from the partial oscillation probability $P_{sin\delta}^{ab}(\Delta_L, \hat{A})$ given in Eq. (A1). We have made no attempt to simplify $P_{sin\delta}^{ab}(\Delta_L, \hat{A})$ because the exact expression for $P_{sin\delta}^{ab}(\Delta_L, \hat{A})$ is already quite simple in form. Expressions for $P^{+ab}(\Delta_L, \hat{A})$ are found in Appendix VI.

Above the solar resonance region, we use the α -expanded representation of \hat{E}_ℓ to obtain our simplified $P^{+ab}(\Delta_L, \hat{A})$. This α -expanded representation appears both in Ref. [1] and in an appendix of Ref. [11].

1. The Bessel functions $j_0^2(\Delta_L \Delta\hat{E}[\ell])$ and \hat{D}

Above the solar resonance resonance, we found it necessary to retain both the first and second terms of the Taylor series expansion of the eigenvalue difference, *i.e.*, $\Delta\hat{E}[\ell] = \Delta\hat{E}_0[\ell](1+r[\ell])$, where $\Delta\hat{E}_0[\ell]$ is the first term of the expansion of $\Delta\hat{E}[\ell]$ in α appearing in Appendix IV C, and $\Delta\hat{E}_0[\ell]r[\ell]$ is the second.

Accordingly, the Bessel functions are expressed,

$$j_0^2(\Delta_L \Delta\hat{E}[\ell]) = \frac{\sin^2 \Delta_L \Delta\hat{E}_0[\ell](1+r[\ell])}{\Delta\hat{E}_0^2[\ell](1+r[\ell])}. \quad (51)$$

Equation (51) may be expanded in $r[\ell]$ using Eq. (17). Equation (17) is an excellent approximation for values of Δ_L appropriate above the solar resonance region, and some may find the expanded form more convenient. All results shown in this section use the expanded form.

Because we find it necessary to retain both the first and the second leading terms of the eigenvalue differences, *i.e.*, $\Delta\hat{E}[\ell] = \Delta\hat{E}_0[\ell](1+r[\ell])$, the energy denominator \hat{D} becomes,

$$\hat{D} = \hat{C}_\alpha(\hat{A} - \alpha(c_{12} + \hat{A}(c_{12} + R_p))) . \quad (52)$$

B. Lower Transition Region, $0.1 < \hat{A} < 0.35$

For the lower transition region, $0.1 < \hat{A} < 0.35$, we find it necessary to make a correction $\delta P^{+e\mu}(\Delta_L, \hat{A})$ that depends on both an effective $\delta\hat{w}_0^{e\mu}[\ell]$ and an effective $\delta\hat{w}_{\cos}^{e\mu}[\ell]$. This correction must be added to $\hat{w}_{\cos}^{e\mu}[\ell]$, which is defined in Table VII. in order to accurately describe the dependence of $P^{+e\mu}(\Delta_L, \hat{A})$ on Δ_L . Consequently, the corrected $P^{(+e\mu)}(\Delta_L, \hat{A})$ becomes a bit more complicated below $\hat{A} = 0.35$ and acquires a sensitivity to δ_{cp} .

By including $\delta P^{+ab}(\Delta_L, \hat{A})$, the accuracy of the corrected $P^{+ab}(\Delta_L, \hat{A})$ given improves also for some distance into the far solar resonance region. For this reason, the solar resonance region has been redefined in this paper to cover the interval $0 < \hat{A} < 0.1$.

1. Numerical Results

Numerical results for the simplified $P^{+ab}(\Delta_L, \hat{A}) + \delta P^{+ab}(\Delta_L, \hat{A})$ within the lower transition region are presented in this section. The quantity $P^{+ab}(\Delta_L, \hat{A})$ is given in Eq. (7). It is evaluated in terms of $\hat{w}_0^{e\mu}[1]$ from Table VII with $D\hat{w}_0^{e\mu}[1] \rightarrow 0$.

Figure 7 shows the dependence of the simplified $P^{+ab}(\Delta_L, \hat{A}) + \delta P^{+ab}(\Delta_L, \hat{A})$ on \hat{A} and Fig. 8 its dependence on Δ_L . In both figures, the simplified results are compared to the exact result [11].

We see from Fig. 7 that the \hat{A} dependence of the simplified $P^{+e\mu}(\Delta_L, \hat{A})$ and the exact oscillation probability agree moderately well.

Comparing our simplified expression for $P^{+ab}(\Delta_L, \hat{A}) + \delta P^{+ab}(\Delta_L, \hat{A})$ shown in Fig. 7 of this paper to Figs. 4 and 5 of Ref. [11], one sees that the results given here are superior to Freund's patched result and comparable or superior to his

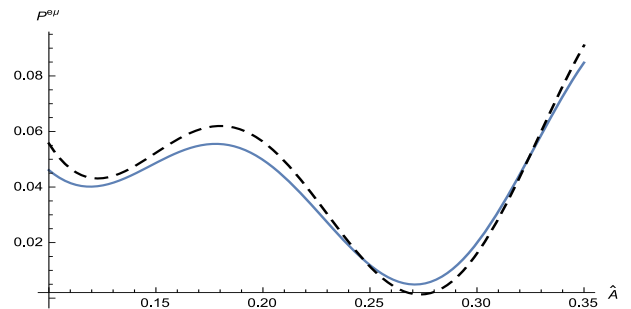


FIG. 7. $P^{+e\mu}(\Delta_L, \hat{A})$ for $\Delta_L = 17$ over the interval $0.1 < \hat{A} < 0.35$ for neutrinos in matter. All parameters are determined by the SNM with $\delta_{cp} = \pi/4$. Exact result (solid curve); simplified result within lower transition region calculated as described above (medium-dashed curve).

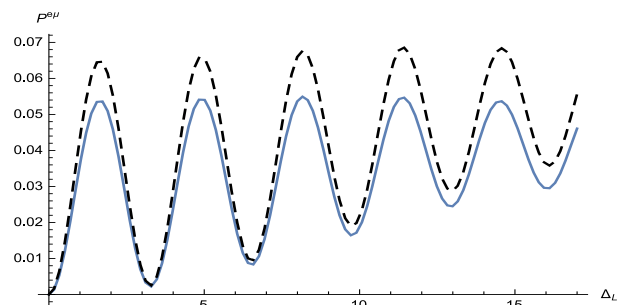


FIG. 8. $P^{+e\mu}(\Delta_L, \hat{A})$ for $\hat{A} = 0.1$ over the interval $0 < \Delta_L < 17$ for neutrinos in matter. All parameters are determined by the SNM with $\delta_{cp} = \pi/4$. Exact result (solid curve); simplified result within lower transition region calculated as described above (medium-dashed curve).

full result over the interval $0.1 < \hat{A} < 0.35$. Our results are definitely superior to the full results of AHLO [9] shown in Figs. 16 and 17 of Ref. [11].

C. Upper Transition Region, $0.35 < \hat{A} < \hat{A}_2$

We next give results we find for the effective oscillation probabilities within the region $0.35 < \hat{A} < \hat{A}_2$. The effective $\hat{w}_0^{e\mu}[\ell]$ is given in Table VII.

1. Numerical Results

Numerical results for the simplified $P^{+ab}(\Delta_L, \hat{A})$ presented in this section are evaluations of Eq. (31) with $\hat{w}_0^{e\mu}[1]$ given in Table VII and, of course,

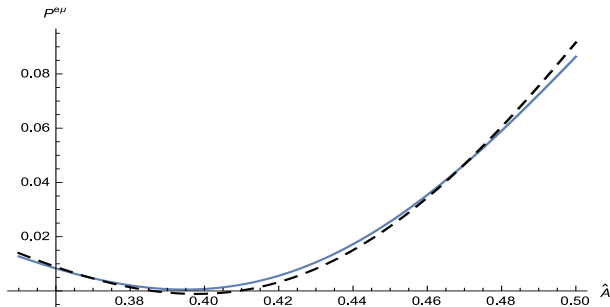


FIG. 9. $P^{+e\mu}(\Delta_L, \hat{A})$ for $\Delta_L = 10$ over the interval $0.35 < \hat{A} < \hat{A}_2$ for neutrinos in matter. All parameters are determined by the SNM. Exact result (solid curve); simplified result within upper transition region calculated as described above (medium-dashed curve).

$D\hat{w}_0^{e\mu}[1] \rightarrow 0$. Figure 9 shows the dependence of the simplified $P^{+ab}(\Delta_L, \hat{A})$ on \hat{A} and Fig. 10 its dependence on Δ_L . In both figures, the simplified results are compared to the exact result [11]. These figures show that both the \hat{A} dependence and the Δ_L dependence of the simplified results compare favorably to the exact results.

Comparing Fig. 9 to results shown in Fig. 5 of Ref. [11], one sees that our simplified results are superior to Freund's patched result throughout the upper transition region and comparable to Freund's full result [11]. Our results are definitely superior to the full results of AHLO [9].

D. Atmospheric Resonance Region:

$$\hat{A}_2 < \hat{A} < 1.2$$

Following Sect. VIC, we find that within the atmospheric resonance region $P^{+e\mu}(\Delta_L, \hat{A})$ has the form given in Eq. (7). The term $D\hat{w}_0^{e\mu}[1]$ is given in Eq. (8 and needed for accuracy within this region, and $\hat{w}_0^{e\mu}[1]$ is given in Table VII. In obtaining this result we found that both of exceptional cases (1) and (2) discussed in Sect. IVA 3 apply to this region.

1. Numerical Results

Figures 10 and 11 show numerical results for the first two leading terms of $P^{+e\mu}(\Delta_L, \hat{A})$ in the region of the atmospheric resonance. We see here that the dependence of $P^{+e\mu}(\Delta_L, \hat{A})$ on both Δ_L and \hat{A} agree well with the exact oscillation probability within this

region.

Figure 6 of Ref. [11] compares the \hat{A} dependence of the full oscillation probability of Freund to that of the oscillation probability of our formulation evaluated with α -expanded eigenvalues. From this comparison, we see that the full oscillation probability of Freund is discontinuous at the position of the atmospheric resonance. Putting this together with Fig. 10 leads to the conclusion that the first two leading terms of our simplified oscillation probability is in better agreement with the exact oscillation probability than the full oscillation probability of Freund.

Additionally, as suggested by Fig. 11, the Δ_L dependence of our simplified oscillation probability agrees well with that of the exact oscillation probability both above and below the atmospheric resonance,

Additionally, we have found that below the atmospheric resonance the Δ_L dependence of Freund's full result [8] agrees well with the Δ_L dependence of the oscillation probability of our formulation with α -expanded eigenvalues, with its magnitude agreeing with that of the oscillation probability of our formulation with α -expanded eigenvalues.

Above the atmospheric resonance, the Δ_L dependence of our simplified oscillation probability agrees well with the Δ_L dependence of the oscillation probability of our formulation with α -expanded eigenvalues, but its magnitude exceeds that of the oscillation probability of our formulation with α -expanded eigenvalues.

Figure 6 of Ref. [11] shows that within the atmospheric resonance region the patched oscillation probability and the full AHLO oscillation probability are significantly larger than the exact oscillation probability and, for this reason, we conclude that Freund's patched oscillation probability and the full AHLO oscillation probability need not be seriously considered further in the atmospheric resonance region.

E. Asymptotic Region: $\hat{A} > 1.2$

We next give results we find for the effective oscillation probabilities within the region $\hat{A} > 1.2$. The procedure given in Sect. IV applied within the asymptotic region once again leads to an expression for $P^{+e\mu}(\Delta_L, \hat{A})$ having the same form that it has in the upper transition region, Eq. (7). The effective $\hat{w}_i^{e\mu}[\ell]$ is given in Table VII and, of course, $D\hat{w}_0^{e\mu}[1] \rightarrow 0$.

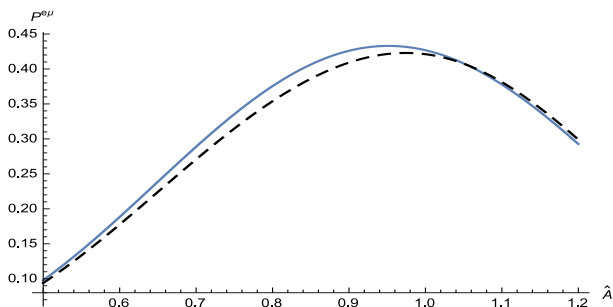


FIG. 10. $P^{+e\mu}(\Delta_L, \hat{A})$ for $\Delta_L = 4$ over the interval $\hat{A}_2 < \hat{A} < 1.2$ for neutrinos in matter. All parameters are determined by the SNM. Exact result (solid curve); simplified result within atmospheric resonance region calculated as described above (medium-dashed curve).

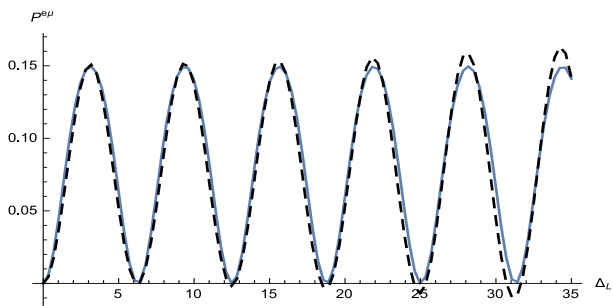


FIG. 11. $P^{+e\mu}(\Delta_L, \hat{A})$ for $\hat{A} = 0.8$ over the interval $0 < \Delta_L < 35$ for neutrinos in matter. All parameters are determined by the SNM. Exact result (solid curve); simplified result within upper transition region calculated as described above (medium-dashed curve).

1. Numerical Results

Figures 12 and 13 show $P^{+e\mu}(\Delta_L, \hat{A})$ compared to the exact oscillation probability as a function of \hat{A} and Δ_L , respectively, within the asymptotic region. We see from these figures that $P^{+e\mu}(\Delta_L, \hat{A})$ and the exact oscillation probability agree to a high level of accuracy within this region.

As before, the other point of interest is again the extent to which $P^{+e\mu}(\Delta_L, \hat{A})$ is an improvement over the familiar approximate formulations. This may be assessed by comparing the \hat{A} and Δ_L dependences of the present theory and the full oscillation probability of Freund.

This assessment of their \hat{A} dependence follows from a comparison of Fig. 12 to Fig. 7 of Ref. [11], which shows Freund's full oscillation probability and

the exact oscillation probability as a function of \hat{A} . Comparing Fig. 12 to Fig. 7 of Ref. [11], one sees that Freund's full oscillation probability is a very good description of the exact result in the asymptotic region. This indicates that our simplified $P^{+e\mu}(\Delta_L, \hat{A})$ offers very little advantage over Freund's full oscillation probability.

An assessment of the Δ_L dependence requires a comparison of the Δ_L dependence of Freund's full oscillation probability and the exact oscillation probability. We have made such a comparison for $\hat{A} = 1.2$ over the interval $1.2 < \Delta_L < 20$ finding that Freund's full oscillation probability agrees very well with the exact oscillation probability.

The Δ_L dependence our simplified $P^{+e\mu}(\Delta_L, \hat{A})$ agrees less well with the exact oscillation probability within the asymptotic region by about 10% than does Freund's full result near the peaks of $P^{+e\mu}(\Delta_L, \hat{A})$. Otherwise, the two agree comparably as well. Whether or not one adopts our simplified $P^{+e\mu}(\Delta_L, \hat{A})$ is therefore a matter of whether this 10% difference is significant for the intended purpose.

Figure 7 of Ref. [11] shows that within the asymptotic region the patched oscillation probability of Freund is significantly larger than the exact oscillation probability and, for this reason, we conclude that Freund's patched oscillation probability need not be seriously considered further in the asymptotic region.

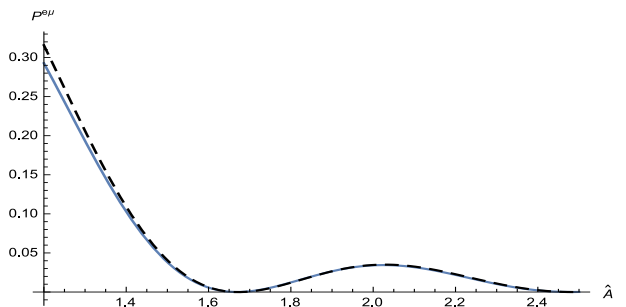


FIG. 12. $P^{+e\mu}(\Delta_L, \hat{A})$ for $\Delta_L = 4$ over the interval $1.2 < \hat{A} < 2.5$ for neutrinos in matter. All parameters are determined by the SNM. Exact result (solid curve); simplified result within asymptotic region calculated as described above (medium-dashed curve).

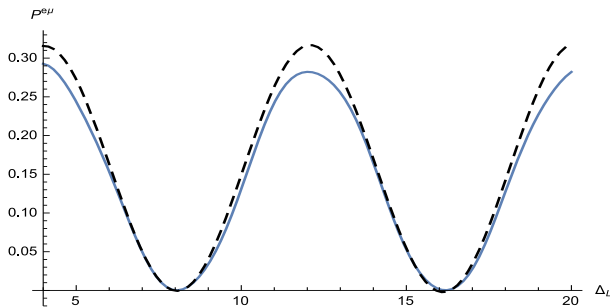


FIG. 13. $P^{+e\mu}(\Delta_L, \hat{A})$ for $\hat{A} = 1.2$ over the interval $4 < \Delta_L < 20$ for neutrinos in matter. All parameters are determined by the SNM. Exact result (solid curve); simplified result within asymptotic region calculated as described above (medium-dashed curve).

F. Discussion

We have found the remarkable result in this section that $\hat{w}_0^{e\mu}[1]$ vanishes in all regions above the lower transition region. Accordingly, we establish an important result, namely that $P^{+ab}(\Delta_L, \hat{A})$ is almost completely independent of the CP violating phase, δ_{cp} , for $\hat{A} > 0.35$.

Another important result is that the expressions we find for $P^{(+e\mu)}(\Delta_L, \hat{A})$ are very accurate above the solar resonance region. These expressions are identical for the first two leading of $\hat{w}_0^{e\mu}[1]$ in all regions except for the lower transition region and the vicinity of the atmospheric resonance. These expressions are also very simple for $\hat{A} > 0.35$. They are given in Table VII. Above the lower transition region, we find, of course, that the effective $P_{cos}^{ab}(\Delta_L, \hat{A})$ vanishes.

Within the lower transition region, the correction term contains both effective $\hat{w}_0^{e\mu}[\ell]$ and effective $\hat{w}_{cos}^{e\mu}[\ell]$ leading to more complicated expressions for $P^{+ab}(\Delta_L, \hat{A})$ and showing that it begins to acquire a sensitivity to δ_{cp} within this region.

It should be emphasized that only in a few instances are these effective partial oscillation probabilities suitable approximations to the exact ones, even though the symmetric oscillation probability $P^{+ab}(\Delta_L, \hat{A})$ obtained by summing the three effective ones as in Eq. (31) does satisfy our accuracy goal. This discussion highlights the fact that even though determination of simple and accurate expressions is purely algebraic, finding the *simplest* expressions is hardly a trivial process.

VII. SUMMARY AND CONCLUSIONS

In this paper, we have determined simple and accurate algebraic expressions for the observable oscillation probabilities characterizing three coupled Dirac neutrinos described by the SNM and convenient for quantitative predictions and analyses of high quality data becoming available at new neutrino facilities. The expressions we found are based on our recently published Hamiltonian formulation.

The procedure leading to our simple and accurate expressions for the oscillation probabilities relies on two main ideas. The first is that many terms constituting the coefficients $w_{i,p}^{(ab)}$ of our original Hamiltonian formulation [11] are small enough to be neglected because of subtle cancellations that occur among these coefficients. We determined a transformation for all transitions $\nu_a \rightarrow \nu_b$ that led to a new set of coefficients $w_{i,p}^{(ab)}$. These are essential for obtaining simple results for the oscillation probability accurate to $O(\alpha^2)$ because they are devoid of such cancellations. The second main idea forms the basis of an efficient and general procedure leading to the *simplest* expressions for oscillation probabilities accurate to $O(\alpha^2)$.

The methods established here are general. Simple and accurate expressions for the neutrino oscillation probabilities for all $\nu_a \rightarrow \nu_b$ transitions are easily obtained with the information given in the appendix of this paper.

We illustrated this procedure and calibrated its for the specific case of $\nu_e \leftrightarrow \nu_\mu$ transitions. These transitions correspond to the experimental situation for which data exists and are the only transitions for which analytic results have been attempted in the literature.

Figures presented in the present paper established the accuracy and reliability of our simple algebraic expressions for the observable oscillation probabilities. Our results are vastly more accurate than results that have been available in the literature for some time throughout the entire region of interest at present and envisioned future neutrino facilities. This accuracy is adequate for analysis and prediction of experiments being considered at future neutrino facilities. Our expressions are only slightly more complicated than the familiar ones.

Our result relies on neutrino mass eigenvalues evaluated using first-order perturbation theory in one of the small parameters $\xi = (\alpha, \sin^2 \theta_{13})$ of the SNM. Within the solar resonance region, the simplest expressions accurate to $O(\alpha^2)$ are based on the

$\sin^2 \theta_{13}$ -expanded eigenvalues, and above the solar resonance region they are based on the α -expanded eigenvalues.

Alternatively, even more accurate results follow using this information in conjunction with a numerical evaluation of the neutrino mass eigenvalues,

which are easily obtained as the solution of a cubic equation. Because this method lacks a fully analytic representation, it is less useful than the analytic result, since, as in the case for all numerical solutions, it is more difficult to obtain insight into the physics in this way.

Appendix A: Our Formulation

Our formulation [1] gives explicit, analytic expressions for the partial oscillation probabilities in terms of the mixing angles, \hat{A} , and the neutrino eigenvalues, \hat{E}_ℓ .

1. Full Oscillation Probability in Our Formulation

One of the partial oscillation probabilities, $P_{\sin \delta}^{ab}$, is antisymmetric under $a \leftrightarrow b$,

$$P_{\sin \delta}^{ab}(\Delta_L, \hat{A}) = \sin \delta_{cp} \Delta_L^3 \alpha (1 - \alpha) (-1)^{a+b} \cos \theta_{13} \sin 2\theta_{12} \sin 2\theta_{13} \sin 2\theta_{23} \Pi_\ell j_0(\Delta_L \Delta \hat{E}[\ell]) . \quad (\text{A1})$$

The other three are individually symmetric,

$$\begin{aligned} P_{\cos \delta}^{ab}(\Delta_L, \hat{A}) &= -\cos \delta_{cp} \frac{4\Delta_L^2}{\hat{D}} \sum_\ell (-1)^\ell \hat{w}_{\cos}^{ab}[\ell] j_0^2(\Delta_L \Delta \hat{E}[\ell]) \\ P_{\cos^2 \delta}^{ab}(\Delta_L, \hat{A}) &= -\cos^2 \delta_{cp} \frac{4\Delta_L^2}{\hat{D}} \sum_\ell (-1)^\ell \hat{w}_{\cos^2}^{ab}[\ell] j_0^2(\Delta_L \Delta \hat{E}[\ell]) \\ P_0^{ab}(\Delta_L, \hat{A}) &= -\frac{4\Delta_L^2}{\hat{D}} \sum_\ell (-1)^\ell \hat{w}_0^{ab}[\ell] j_0^2(\Delta_L \Delta \hat{E}[\ell]) , \end{aligned} \quad (\text{A2})$$

where the sum runs over $\ell = 1, 2, 3$,

$$\hat{D} = \Delta \hat{E}[1] \Delta \hat{E}[2] \Delta \hat{E}[3] , \quad (\text{A3})$$

and, the quantity Δ_L appearing in Eqs. (A1,A2) is defined in Eq. (25). In Eq.(A2),

$$\hat{w}_i^{ab}[\ell] = (w_{i;0}^{(ab)} + w_{i;1}^{(ab)} \hat{E}_\ell + w_{i;2}^{(ab)} \hat{E}_\ell^2) \Delta \hat{E}[\ell] . \quad (\text{A4})$$

The bracket notation is the same as that used throughout our work [1].

The total oscillation probability for neutrinos is then,

$$\begin{aligned} \mathcal{P}(\nu_b \rightarrow \nu_a) &= \delta(a, b) + P_0^{ab} + P_{\sin \delta}^{ab} + P_{\cos \delta}^{ab} \\ &\quad + P_{\cos^2 \delta}^{ab} . \end{aligned} \quad (\text{A5})$$

Because the masses are ordered so that $m_3 > m_2 > m_1$ and eigenvalues do not cross, it follows that $\hat{E}_3 > \hat{E}_2 > \hat{E}_1$ for all $|\hat{A}|$. Consequently, $\Delta \hat{E}[\ell]$ as well as \hat{D} are all positive.

The partial oscillation probabilities in Eqs. (A1,A2) have been expressed as explicit functions of Δ_L and \hat{A} to indicate that the entire dependence on the neutrino beam energy E , the baseline L , and the medium properties occurs through Δ_L and \hat{A} . This follows from their definitions in Eqs. (9,25), respectively.

The matrices $w_{i;n}^{ab}$ appearing in Eq. (A2) take the form [1].

$$w_{\cos^2;n} = \sin^2 2\theta_{23} \begin{pmatrix} 0 & 0 & 0 \\ 0 & w_{\cos^2;n}^{(22)} & -w_{\cos^2;n}^{(22)} \\ 0 & -w_{\cos^2;n}^{(22)} & w_{\cos^2;n}^{(22)} \end{pmatrix}, \quad (\text{A6})$$

$$w_{\cos;n} = \sin 2\theta_{23} \begin{pmatrix} 0 & w_{\cos;n}^{(12)} & -w_{\cos;n}^{(12)} \\ w_{\cos;n}^{(12)} & w_{\cos;n}^{(22)} & w_{\cos;n}^{(23)} \\ -w_{\cos;n}^{(12)} & w_{\cos;n}^{(23)} & w_{\cos;n}^{(33)} \end{pmatrix}, \quad (\text{A7})$$

and

$$w_{0;n} = \begin{pmatrix} w_{0;n}^{(11)} & w_{0;n}^{(12)} & w_{0;n}^{(13)} \\ w_{0;n}^{(12)} & w_{0;n}^{(22)} & w_{0;n}^{(23)} \\ w_{0;n}^{(13)} & w_{0;n}^{(23)} & w_{0;n}^{(33)} \end{pmatrix}. \quad (\text{A8})$$

The partial oscillation probabilities given in Eqs. (A1,A2) are *exact* when evaluated in terms of the exact eigenvalues [see Eq. (40) of Ref [1]] and the full expressions for the coefficients $w_{i;n}^{(ab)}$ [see Appendix C of Ref [11]].

The usefulness of the oscillation probabilities follows from various interconnections among them. One of these is that the exchange of initial and final states in the oscillation probability of neutrinos (antineutrinos) is equivalent to letting $\delta_{cp} \rightarrow -\delta_{cp}$. Thus, the result for the inverse reaction $\mathcal{P}(\nu_b \rightarrow \nu_a)$ is found by exchanging (a, b) in Eq. (A5). Since $P_{\sin \delta}^{ab}$ is antisymmetric under the exchange of (a, b) , and P_0^{ab} , $P_{\cos \delta}^{ab}$ and $P_{\cos^2 \delta}^{ab}$ symmetric, it follows that P^{ba} is given by

$$\begin{aligned} \mathcal{P}(\nu_b \rightarrow \nu_a) &= \delta(a, b) + P_0^{ab} - P_{\sin \delta}^{ab} + P_{\cos \delta}^{ab} \\ &\quad + P_{\cos^2 \delta}^{ab}. \end{aligned} \quad (\text{A9})$$

In analogy to Eq. (A5), we may express the oscillation probability for antineutrinos as

$$\begin{aligned} \mathcal{P}(\bar{\nu}_a \rightarrow \bar{\nu}_b) &\equiv \bar{P}^{ab}(\Delta_L, \hat{A}) \\ &= \delta(a, b) + \bar{P}_0^{ab} + \bar{P}_{\sin \delta}^{ab} + \bar{P}_{\cos \delta}^{ab} + \bar{P}_{\cos^2 \delta}^{ab}, \end{aligned} \quad (\text{A10})$$

where the bared probabilities for anti neutrinos are obtained from the unbarred for neutrinos by replacing $\delta_{cp} \rightarrow -\delta_{cp}$ and $\hat{A} \rightarrow -\hat{A}$. Because the energies of antineutrinos are different from those of the neutrinos in matter, we can expect $P^{ab} \neq \bar{P}^{ab}$ in this situation.

Again applying the rule that exchange of initial and final states is accomplished by letting $\delta_{cp} \rightarrow -\delta_{cp}$, the oscillation probability $\mathcal{P}(\bar{\nu}_b \rightarrow \bar{\nu}_a)$ is expressed in terms of the same four quantities,

$$\begin{aligned} \mathcal{P}(\bar{\nu}_b \rightarrow \bar{\nu}_a) &= \delta(a, b) + \bar{P}_0^{ab} - \bar{P}_{\sin \delta}^{ab} + \bar{P}_{\cos \delta}^{ab} + \bar{P}_{\cos^2 \delta}^{ab}. \end{aligned} \quad (\text{A11})$$

Appendix B: Approximate Oscillation Probability in Our Formulation

As discussed in Sect. III, many terms constituting the exact expressions for coefficients $w_{i,p}^{(ab)}$, which are given explicitly in Appendix C of Ref. [11], are small and may be neglected without compromising the overall reliability of our result. However, it is not straightforward to recognize the cancelling terms because of subtle cancellations that occur among these coefficients. The source of these cancellations is identified in Sect. III B above and, based on this understanding, we determine a transformation leading to a new set of coefficients $w_{i,p}^{(ab)}$,

$$\hat{w}_i^{ab}[\ell] = (w_{i;0^-}^{(ab)} + w_{i;1^-}^{(ab)}(\hat{E}_\ell - 1) + w_{i;2^-}^{(ab)}\hat{E}_\ell(\hat{E}_\ell - 1))\Delta\hat{E}[\ell] , \quad (\text{B1})$$

which are devoid of cancellations. The first two leading terms of the coefficients $w_{i;p^-}^{(ab)}$ are essential for obtaining simple results for the oscillation probability accurate to $O(\alpha^2)$. These coefficients are tabulated below for all transitions $\nu_a \rightarrow \nu_b$. The expressions for the approximate oscillation probability are those given in Eqs. (A1,A2), but with $w_{i;p^-}^{ab}[\ell]$ evaluated using the first two leading terms of the coefficients $\hat{w}_{i;p^-}^{(ab)}$. The overall factor K_{ab}^i of each coefficient $\hat{w}_{i;p^-}^{(ab)}$ appears in Table I. The actual coefficient $w_{i;p^-}^{(ab)}$ are found from those given below by multiplying them by K_{ab}^i ,

$$w_{i;p^-}^{(ab)} \rightarrow K_{ab}^i w_{i;p^-}^{(ab)} . \quad (\text{B2})$$

Appendix C: First Two Leading Terms of the Coefficients $w_{i;p^-}^{(ab)}$

The first two leading terms of the coefficients $w_{\cos^2,p^-}^{(ab)}$ are given in Sect. C 1; those for $w_{\cos,p^-}^{(ab)}$ in Sect. C 2; and, those for $w_{0,p^-}^{(ab)}$ in Sect. C 3.

1. $w_p^{(22)}(i = \cos^2)$

$$\begin{aligned} w_{\cos^2,0^-}^{(22)} &= (1 - \alpha + \hat{A}(1 - \alpha(s_{12}^2 + R_p))) \\ w_{\cos^2,1^-}^{(22)} &= (1 - \alpha) \\ w_{\cos^2,2^-}^{(22)} &= 1 . \end{aligned} \quad (\text{C1})$$

The remaining coefficients $w_{\cos^2,p^-}^{(ab)}$ are found from these as follows,

$$\begin{aligned} w_{\cos^2,p^-}^{(23)} &= w_{\cos^2,p^-}^{(32)} = -w_{\cos^2,p^-}^{(22)} \\ w_{\cos^2,p^-}^{(33)} &= w_{\cos^2,p^-}^{(22)} \\ w_{\cos^2,p^-}^{(11)} &= w_{\cos^2,p^-}^{(12)} = w_{\cos^2,p^-}^{(13)} = w_{\cos^2,p^-}^{(21)} \\ &= w_{\cos^2,p^-}^{(31)} = 0 , \end{aligned} \quad (\text{C2})$$

2. $w_p^{(12)}$, $w_p^{(23)}$, and $w_p^{(22)}(i = \cos)$

$$\begin{aligned} w_{\cos,0^-}^{(12)} &= \alpha(c_{12}^2 - s_{12}^2)(1 - \alpha(1 + R_p)) - \hat{A}(1 - \alpha(1 + R_p)) \\ w_{\cos,1^-}^{(12)} &= (1 - \alpha(1 + 2s_{12}^2 + R_p)) - \hat{A}w_{\cos,2^-}^{(12)} \\ w_{\cos,2^-}^{(12)} &= (1 - \alpha(s_{12}^2 + R_p)) ; \end{aligned} \quad (\text{C3})$$

$$\begin{aligned} w_{\cos,0^-}^{(23)} &= c_{12}s_{12}(\alpha(c_{12}^2 - s_{12}^2) - \alpha^2(1 - R_p)) \\ &\quad \times (c_{12}^2 - s_{12}^2)(c_{23}^2 - s_{23}^2) - \hat{A}(1 - \alpha(1 + 3R_p)) \\ w_{\cos,1^-}^{(23)} &= -c_{12}(1 - \alpha(1 + 2c_{12}^2 + R_p))s_{12}(c_{23}^2 - s_{23}^2) \\ w_{\cos,2^-}^{(23)} &= -2c_{12}s_{12}(1 - \alpha(c_{12}^2 + R_p))(c_{23}^2 \\ &\quad - s_{23}^2) ; \end{aligned} \quad (\text{C4})$$

and,

$$\begin{aligned}
w_{\cos;0-}^{(22)} &= \alpha c_{23}^2 (c_{12}^2 - s_{12}^2) - \alpha^2 (c_{12}^2 - s_{12}^2) (c_{23}^2 + R_p s_{23}^2) \\
&\quad - \hat{A} (c_{23}^2 - \alpha (c_{23}^2 + R_p (1 - 3s_{23}^2))) \\
w_{\cos;1-}^{(22)} &= -\hat{A} (1 - \alpha (s_{12}^2 + R_p)) + s_{23}^2 + \alpha (c_{12}^2 - s_{12}^2) \\
&\quad - s_{23}^2 (1 + 2c_{12}^2 + R_p) \\
w_{\cos;2-}^{(22)} &= 2s_{23}^2 + \alpha (c_{23}^2 - 2c_{23}^2 s_{12}^2 - s_{23}^2 - 2R_p) \\
&\quad \times s_{23}^2 .
\end{aligned} \tag{C5}$$

The remaining coefficients $w_{\cos,p-}^{(ab)}$ are found from these as follows,

$$\begin{aligned}
w_{\cos,p-}^{(13)} &= w_{\cos,p-}^{(31)} = -w_{\cos,p-}^{(12)} \\
w_{\cos,p-}^{(21)} &= w_{\cos,p-}^{(12)} .
\end{aligned} \tag{C6}$$

The coefficients $w_{\cos,p-}^{(33)}$ are obtained from $w_{\cos,p-}^{(22)}$ by making the replacement $\sin \theta_{23} \leftrightarrow \cos \theta_{23}$ and flipping the overall sign.

3. $w_p^{(12)}$, $w_p^{(23)}$, $w_p^{(11)}$ and $w_p^{(22)}$ ($i = 0$)

$$\begin{aligned}
w_{0;0-}^{(12)} &= \alpha (4s_{12}^2 c_{12}^2 (c_{23}^2 - \alpha (c_{23}^2 + R_p)) - \hat{A} (4c_{12}^2 c_{23}^2 s_{12}^2 + 4R_p^2 s_{23}^2 - \alpha (4c_{12}^4 c_{23}^2 s_{12}^2 - R_p s_{23}^2 (4c_{12}^2 s_{12}^2 - 12R_p s_{12}^2 - 4R_p^2)))) \\
w_{0;1-}^{(12)} &= (4\alpha s_{12}^2 (c_{12}^2 c_{23}^2 - R_p s_{23}^2) - \alpha^2 s_{12}^2 (4c_{12}^2 c_{23}^2 + 4R_p (c_{23}^2 - s_{12}^2 - s_{23}^2 - R_p s_{23}^2))) - \hat{A} w_{0;2-}^{(12)} \\
w_{0;2-}^{(12)} &= 4R_p s_{23}^2 + \alpha (4c_{12}^2 c_{23}^2 s_{12}^2 - 4R_p (R_p + 2s_{12}^2) s_{23}^2) ;
\end{aligned} \tag{C7}$$

$$\begin{aligned}
w_{0;0-}^{(23)} &= -\alpha (16\alpha c_{12}^2 c_{23}^2 s_{12}^2 s_{23}^2 + 4s_{23}^2 c_{23}^2 \hat{A} (4R_p - \alpha (4c_{12}^2 s_{12}^2 + 4R_p (1 + 2R_p + s_{12}^2)))) \\
&\quad - \alpha^2 (16c_{12}^2 c_{23}^2 s_{12}^2 s_{23}^2 + 2R_p (8c_{12}^2 s_{12}^2 + 8c_{23}^2 s_{23}^2 - 16c_{12}^2 c_{23}^2 s_{12}^2 s_{23}^2)) \\
w_{0;1-}^{(23)} &= -16\alpha s_{23}^2 c_{23}^2 (c_{12}^2 - \alpha (c_{12}^2 + c_{12}^4 + R_p)) \\
w_{0;2-}^{(23)} &= 16c_{23}^2 s_{23}^2 (1 - 2\alpha (c_{12}^2 + R_p)) ;
\end{aligned} \tag{C8}$$

$$\begin{aligned}
w_{0;0-}^{(11)} &= -4\alpha s_{12}^2 c_{12}^2 (1 - \alpha (1 + 2R_p)) \\
w_{0;1-}^{(11)} &= -4\alpha s_{12}^2 (c_{12}^2 - R_p - \alpha (c_{12}^2 - R_p (R_p + 2s_{12}^2))) \\
w_{0;2-}^{(11)} &= -4R_p - \alpha (4c_{12}^2 s_{12}^2 - 4R_p (R_p + 2s_{12}^2)) ;
\end{aligned} \tag{C9}$$

and,

$$\begin{aligned}
w_{0;0-}^{(22)} &= \alpha (4\alpha c_{23}^4 c_{12}^2 s_{12}^2 - \alpha^2 c_{23}^2 (4c_{12}^2 c_{23}^2 s_{12}^2 - 2R_p s_{23}^2 (1 + (c_{12}^2 - s_{12}^2)^2)) - \hat{A} (4R_p c_{23}^2 s_{23}^2 \\
&\quad + \alpha (4c_{12}^2 c_{23}^2 s_{12}^2 - 4R_p s_{23}^2 (c_{23}^2 (1 + s_{12}^2) + R_p (c_{23}^2 - s_{23}^2)))) \\
w_{0;1-}^{(22)} &= \alpha (4c_{12}^2 c_{23}^2 s_{12}^2 - \alpha (2R_p s_{23}^2 (c_{12}^2 + c_{23}^2 - s_{12}^2 - s_{23}^2 + c_{12}^2 c_{23}^2 (1 + 2s_{12}^2 + 6s_{23}^2 - (c_{12}^2 - s_{12}^2) (c_{23}^2 - s_{23}^2)))) \\
&\quad + 4\hat{A} (R_p s_{23}^2 + \alpha (c_{12}^2 c_{23}^2 s_{12}^2 - R_p (R_p + 2s_{12}^2) s_{23}^2))) \\
w_{0;2-}^{(22)} &= -4s_{23}^2 (c_{23}^2 - \alpha (2c_{12}^2 c_{23}^2 + R_p (c_{23}^2 - s_{23}^2)))
\end{aligned} \tag{C10}$$

The remaining coefficients $w_{0,p^-}^{(ab)}$ are obtained from these as follows,

$$\begin{aligned} w_{0,p^-}^{(21)} &= w_{0,p^-}^{(31)} \\ &= w_{0,p^-}^{(12)} . \end{aligned} \tag{C11}$$

The coefficients $w_{0,p^-}^{(33)}$ are obtained from $w_{0,p^-}^{(22)}$ by making the replacement $\sin \theta_{23} \leftrightarrow \cos \theta_{23}$. Likewise, $w_{0,p^-}^{(13)}$ are obtained from $w_{0,p^-}^{(12)}$ the same way, making the same replacement, $\sin \theta_{23} \leftrightarrow \cos \theta_{23}$.

TABLE I. Coefficients K_{ab}^i of the coefficients $w_{i;p^-}^{(ab)}$

| i | (a,b) | K_{ab}^i |
|-------|--------|--|
| c_2 | (2, 2) | $\alpha^3 R_p s_{12}^2 c_{12}^2$ |
| c | (1, 2) | $\alpha \frac{\sqrt{\alpha R_p}}{2} s_{12} c_{12}$ |
| c | (2, 3) | $\alpha \sqrt{\alpha R_p} s_{12}^2 c_{12}^2$ |
| c | (2, 2) | $-\alpha \sqrt{\alpha R_p} s_{12} c_{12}$ |
| 0 | (1, 2) | $\frac{\alpha}{4}$ |
| 0 | (2, 3) | $\frac{1}{16}$ |
| 0 | (1, 1) | $\frac{\alpha}{4}$ |
| 0 | (2, 2) | $\frac{1}{4}$ |

IV. SMALL PARAMETER EXPANSIONS

We have shown [1] that expansions of the eigenvalues in the small parameter α is troublesome in the vicinity of the solar resonance and that expansions of the eigenvalues in the small parameter $\sin^2 \theta_{13}$ is troublesome in the vicinity of the atmospheric resonance. These problems are avoided in this paper by expressing the oscillation probability within the solar resonance region by using the expansion of the eigenvalues in $\sin^2 \theta_{13}$ and above the solar resonance region by using the expansion of the eigenvalues in α .

A. Quantities $\Delta \hat{E}_0[\ell]$ and $r[\ell]$

In this section, we define the energy differences $\Delta \hat{E}_0[\ell]$ and $\Delta \hat{E}_1[\ell]$,

$$\begin{aligned} \Delta \hat{E}_n[1] &= \hat{E}_{n,3} - \hat{E}_{n,2} \\ \Delta \hat{E}_n[2] &= \hat{E}_{n,3} - \hat{E}_{n,1} \\ \Delta \hat{E}_n[3] &= \hat{E}_{n,2} - \hat{E}_{n,1} . \end{aligned} \tag{1}$$

For $n = 0$, $\hat{E}_{n,\ell}$ is the first term of a Taylor expansion in α of the ξ -expanded eigenvalues \hat{E}_ℓ , and for $n = 1$ $\hat{E}_{n,\ell}$ is the second term of the Taylor expansion.

We then define from these $\Delta \hat{E}_0[\ell]$ and $\Delta \hat{E}_1[\ell]$ the quantities $\Delta \hat{E}[\ell]$ and $r[\ell]$,

$$\Delta \hat{E}[\ell] \equiv \Delta \hat{E}_0[\ell] + \Delta \hat{E}_1[\ell]$$

$$= \Delta \hat{E}_0[\ell](1 + r[\ell]) , \quad (2)$$

where, clearly,

$$r[\ell] \equiv \Delta \hat{E}_1[\ell] / \Delta \hat{E}_0[\ell] . \quad (3)$$

The quantities $\Delta \hat{E}_0[\ell]$ and $r[\ell]$ are of course different above and below the solar resonance region.

Because $r[\ell]$ is small parameter, we may consider simplifying the oscillation probability by expanding pieces of it in $r[\ell]$. The quantities we have in mind are the Bessel function, $j_0^2(\hat{\Delta}[\ell])$ and \hat{D} ,

$$\hat{D} \equiv \Delta \hat{E}[1] \Delta \hat{E}[2] \Delta \hat{E}[3] . \quad (4)$$

B. Quantities $\Delta \hat{E}_0[\ell]$ and $r[\ell]$ within the Solar Resonance Region

As discussed, there are advantages to splitting the solar resonance region into two sub-regions. One of these is the deep solar resonance region, $\hat{A} < \alpha$, and the other is the far solar resonance region, $\hat{A} > \alpha$.

$$1. \quad \xi = \sin^2 \theta_{13} , \hat{A} < \alpha$$

For $\hat{A} < \alpha$, we find the following expressions for $\Delta \hat{E}_0[\ell]$,

$$\begin{aligned} (a) \quad \Delta \hat{E}_0[1] &= 1 - \frac{\alpha}{2}(1 + R_s + C_T) \\ (b) \quad \Delta \hat{E}_0[2] &= 1 - \frac{\alpha}{2}(1 + R_s - C_T) \\ (c) \quad \Delta \hat{E}_0[3] &= \alpha C_T \end{aligned} \quad (5)$$

The corresponding parameters $r[\ell]$, defined in Eq. (3), are

$$\begin{aligned} (a) \quad r[1] &= \alpha^2 \frac{R_p R_s (2 + R_s)}{(1 - \alpha R_s)(2 - \alpha(1 + R_s + C_T))} \\ (b) \quad r[2] &= \alpha^2 \frac{R_p R_s (4 - R_s)}{(1 - \alpha R_s)(2 - \alpha(1 + R_s - C_T))} \\ (c) \quad r[3] &= \alpha \frac{R_p R_s (1 - R_s)}{C_T (1 - \alpha R_s)} . \end{aligned} \quad (6)$$

$$2. \quad \xi = \sin^2 \theta_{13} , \hat{A} > \alpha$$

For $\hat{A} > \alpha$, we find,

$$(a) \quad \Delta \hat{E}_0[1] = 1 - \frac{\alpha}{2R_s}(1 + R_s + C_T)$$

$$(b) \quad \Delta \hat{E}_0[2] = 1 - \frac{\alpha}{2R_s}(1 + R_s - C_T)$$

$$(c) \quad \Delta \hat{E}_0[3] = \frac{\alpha}{R_s} C_T \quad (7)$$

and

$$\begin{aligned} (a) \quad r[1] &= -\alpha^2 \frac{3R_s R_p}{(\alpha - R_s)(2R_s - \alpha(1 + R_s + C_T))} \\ (b) \quad r[2] &= -\alpha^2 \frac{3R_s R_p}{(\alpha - R_s)(2R_s - \alpha(1 + R_s - C_T))} \\ (c) \quad r[3] &= 0 . \end{aligned} \quad (8)$$

C. Expressions for $\Delta \hat{E}_0[\ell]$ and $r[\ell]$ Above the Solar Resonance Region

For the α -expanded eigenvalues, we find,

$$\begin{aligned} (a) \quad \Delta \hat{E}_0[1] &= \hat{C}_\alpha \\ (b) \quad \Delta \hat{E}_0[2] &= \frac{1}{2}(1 + \hat{A} + \hat{C}_\alpha) \\ (c) \quad \Delta \hat{E}_0[3] &= \frac{1}{2}(1 + \hat{A} - \hat{C}_\alpha) \end{aligned} \quad (9)$$

and

$$\begin{aligned} (a) \quad r[1] &= -\alpha \frac{s_{12}^2}{\hat{C}_\alpha^2} (1 - \hat{A}) \\ (b) \quad r[2] &= -\alpha \frac{s_{12}^2(1 - \hat{A}) - \hat{C}_\alpha(1 - 3c_{12}^2)}{(1 - \hat{A})^2 + \hat{C}_\alpha(1 - \hat{A}) + 4\alpha \hat{A} R_p} \\ (c) \quad r[3] &= -\alpha \frac{s_{12}^2(1 - \hat{A}) + \hat{C}_\alpha(1 - 3c_{12}^2)}{(1 - \hat{A})^2 - \hat{C}_\alpha(1 - \hat{A}) + 4\alpha \hat{A} R_p} . \end{aligned} \quad (10)$$

V. OBSERVABLE NEUTRINO OSCILLATION PROBABILITIES

In Appendix A, the full neutrino oscillation probability, $\mathcal{P}(\nu_a \rightarrow \nu_b)$, is expressed as the sum of two observable oscillation probabilities. One of these, $P_{\sin \delta}^{ab}$, is anti-symmetric under the exchange $a \leftrightarrow b$ and the other, which we call $P^{+\epsilon\mu}(\Delta_L, \hat{A})$, is symmetric. The anti-symmetric observable given in Eq. (A1) is proportional to $\sin \theta_{cp}$, where δ_{cp} is the CP violating phase. The exact expression for this quantity is sufficiently simple that it requires no further simplification. However, the analytic expression for $P^{+\epsilon\mu}(\Delta_L, \hat{A})$ is rather complicated, and its simplification is the subject of this paper. These $P^{+\epsilon\mu}(\Delta_L, \hat{A})$ have been simplified by region as explained in Sect. IV. In this Appendix we summarize our findings.

A. Regions of \hat{A}

The oscillation probability $P^{+e\mu}(\Delta_L, \hat{A})$ will be given separately for $0 < \hat{A} < 0.1$, which we refer to as the solar resonance region, and the region $\hat{A} > 0.1$. Each of these regions is subdivided into various intervals.

The oscillation probability $P^{+e\mu}(\Delta_L, \hat{A})$ takes quite different forms depending upon the interval of \hat{A} considered. The most complicated expressions for our simplified $P^{+e\mu}(\Delta_L, \hat{A})$ are those describing the lower transition region.

B. Effective $P_{\cos\delta}^{ab}(\Delta_L, \hat{A})$, $P_{\cos^2\delta}^{ab}(\Delta_L, \hat{A})$, and $P_0^{ab}(\Delta_L, \hat{A})$

As discussed in Sect. IV A 3, “effective” partial oscillation probabilities $P_{\cos\delta}^{ab}(\Delta_L, \hat{A})$, $P_{\cos^2\delta}^{ab}(\Delta_L, \hat{A})$, and $P_0^{ab}(\Delta_L, \hat{A})$ may be defined from $P^{+e\mu}(\Delta_L, \hat{A})$. The effective partial oscillation probability $P_{\cos\delta}^{ab}(\Delta_L, \hat{A})$ represents the dependence

of $P^{+ab}(\Delta_L, \hat{A})$ on δ_{cp} ; the effective partial oscillation probability $P_{\cos^2\delta}^{ab}(\Delta_L, \hat{A})$ represents its dependence on δ_{cp}^2 ; and, the effective $P_0^{ab}(\Delta_L, \hat{A})$ its terms independent of δ_{cp} .

These effective partial oscillation determine, in turn, effective $\hat{w}_i^{e\mu}[\ell]$. The expressions for the effective $\hat{w}_i^{e\mu}[\ell]$ are much simpler than the full $\hat{w}_i^{e\mu}[\ell]$, as is the case for the Bessel functions. Note, however, that neither the effective partial oscillation probabilities nor the effective $\hat{w}_i^{e\mu}[\ell]$ are guaranteed to be the simplest to $O(\alpha^2)$.

As we will see, two exceptional cases, described in Sect. IV A 3, apply to both regions of \hat{A} .

VI. SUMMARY OF SIMPLIFIED OSCILLATION PROBABILITIES

In this section, we give the simplified analytic expressions for the effective partial oscillation probabilities $P_{\cos\delta}^{ab}(\Delta_L, \hat{A})$, $P_{\cos^2\delta}^{ab}(\Delta_L, \hat{A})$, and $P_0^{ab}(\Delta_L, \hat{A})$ and the effective $\hat{w}_i^{e\mu}[\ell]$. Results are presented by region.

A. Solar Resonance Region, $0 < \hat{A} < 0.1$

The solar resonance region consists of the deep solar resonance region, $0 < \hat{A} < \alpha$, and the far solar resonance region, $\alpha < \hat{A} < 0.1$. Within this region, our simplified oscillation probability symmetric in $a \leftrightarrow b$ is of the form,

$$P^{+ab}(\Delta_L, \hat{A}) = -\frac{4\Delta_L^2}{\hat{D}} \sum_{i,\ell} (-1)^\ell \hat{w}_i^{ab}[\ell] j_0^2(\Delta_L \Delta \hat{E}[\ell]), \quad (1)$$

where the sum runs over $i = (0, \cos)$. Within the solar resonance region, we find it sufficient to retain only the first leading term of eigenvalue difference, *i.e.*, $\Delta \hat{E}[\ell] = \Delta \hat{E}_0[\ell]$, where $\Delta \hat{E}_0[\ell]$ is given in Appendix IV B.

1. Deep Solar Resonance Region, $0 < \hat{A} < \alpha$

The expressions we find for the effective $\hat{w}_i^{e\mu}[\ell]$ within the deep solar resonance region are given in Table II. We also give the eigenvalue difference $\Delta \hat{E}_0[\ell]$.

2. Far Solar Resonance Region, $\alpha < \hat{A} < 0.1$

Expressions for effective values of $\hat{w}_i^{e\mu}[\ell]$ within the far solar resonance region are given in Table III. The coefficients AA , K_C , and K_0 appearing in Table III are defined as follows,

$$AA \equiv -1 - 3\alpha + \alpha R_p + R_s \cos 2\theta_{12} + 10\alpha s_{12}^2$$

TABLE II. Deep Solar

| Quantity | $\ell = 1$ | $\ell = 2$ | $\ell = 3$ |
|------------------------------|------------------------------------|----------------------------|-------------|
| $\hat{w}_0^{e\mu}[\ell]$ | $K_0(2s_{12}^2 + R_s)$ | $K_0(c_{12}^2 - R_s)$ | 0 |
| $\hat{w}_{cos}^{e\mu}[\ell]$ | $-K_C(1 - \alpha(3 + R_p + 4R_s))$ | $-\hat{w}_{cos}^{e\mu}[1]$ | 0 |
| $\Delta\hat{E}_0[\ell]$ | Eq. (5) (a) | Eq. (5) (b) | Eq. (5) (c) |

$$\begin{aligned}
K_C &\equiv -\cos\delta_{cp}\frac{\alpha\sqrt{\alpha R_p}}{2(\alpha - R_s)^3}s_{12}c_{12} \\
K_0 &\equiv \frac{\alpha^2}{2(\alpha - R_s)^3}R_s.
\end{aligned} \tag{2}$$

TABLE III. $\hat{w}_{cos}^{e\mu}[\ell]$: Far Solar

| Quantity | $\ell = 1$ | $\ell = 2$ | $\ell = 3$ |
|----------------------------------|------------------------------|--|--|
| $\hat{w}_{cos}^{e\mu}[\ell]/K_C$ | $R_s(R_s - 2\alpha)^2$ | $-\hat{w}_{cos}^{e\mu}[1]/K_C$ | $\alpha^2(R_s C_T(1 - R_s \cos 2\theta_{12}) - \alpha(3 + R_s R_p))$ |
| $\hat{w}_0^{e\mu}[\ell]/K_0$ | $R_s R_p s_{23}^2(AA + C_T)$ | $-R_p s_{23}^2(8\alpha + R_s(AA - C_T + 2\alpha R_p))$ | $\alpha s_{12}^2 c_{12}^2(R_s c_{23}^2 C_T - 4\alpha c_{23}^2)$ |
| $\Delta\hat{E}_0[\ell]$ | Eq. (7) (a) | Eq. (7) (b) | Eq. (7) (c) |

B. Above Solar Resonance Region, $\hat{A} > 0.1$

The regions with $\hat{A} > 0.1$ consist of the lower transition region, $0.1 < \hat{A} < 0.35$; the upper transition region, $0.35 < \hat{A} < \hat{A}_2$; the atmospheric resonance region, $\hat{A}_2 < \hat{A} < 1.2$; and, the asymptotic region, $\hat{A} > 1.2$. Within all these regions, we find it necessary to retain both the first and the second leading terms of the eigenvalue differences, *i.e.*, $\Delta\hat{E}[\ell] = \Delta\hat{E}_0[\ell](1 + r[\ell])$.

In all regions above the solar resonance region, except for the lower transition region, our simplified oscillation probability $P^{+ab}(\Delta_L, \hat{A})$ has the same form with just one component,

$$P^{+ab}(\Delta_L, \hat{A}) = \frac{4\Delta_L^2}{\hat{D}}(\hat{w}_0^{ab}[1] + D\hat{w}_0^{e\mu}[1])j_0^2(\Delta_L\Delta\hat{E}[1]). \tag{3}$$

The coefficient $\hat{w}_0^{e\mu}[1]$ is given in Table VII and $D\hat{w}_0^{e\mu}[1]$,

$$D\hat{w}_0^{e\mu}[1] = \frac{2\alpha^2 R_p^2}{\hat{C}_\alpha} s_{23}^2(3c_{12}^2 + 4R_p), \tag{4}$$

is a correction required for accuracy in the atmospheric resonance region.

The Bessel function in Eq. (7) simplified by using its expanded representation given in Eq. (17) below and taking $\Delta\hat{E}[1]$ from Table VII. We find,

$$P^{+ab}(\Delta_L, \hat{A}) = \frac{4\Delta_L^2}{\hat{D}}((\hat{w}_0^{ab}[1] + D\hat{w}_0^{e\mu}[1])j_0^2(\Delta_L\hat{C}_\alpha) + 2r[\ell]\hat{w}_0^{ab}[1](j_0(2\Delta_L\hat{C}_\alpha) - j_0^2(\Delta_L\hat{C}_\alpha))), \tag{5}$$

where the term $r[\ell]D\hat{w}_0^{e\mu}[1]$ has been dropped because it is of order α^3 and therefore quite small. The short-hand notation $\tilde{A} \equiv 1 - \hat{A}$ is used in Table VII and below for the frequently occurring quantity $1 - \hat{A}$.

1. The Lower Transition Region

Within the lower transition region, our simplified oscillation probability symmetric under $a \leftrightarrow b$ consists of two pieces $P^{+ab}(\Delta_L, \hat{A})$ and $\delta P^{+ab}(\Delta_L, \hat{A})$, where $P^{+ab}(\Delta_L, \hat{A})$ is given in Eq. (1), and $\delta P^{+ab}(\Delta_L, \hat{A})$ is,

$$\delta P^{+ab}(\Delta_L, \hat{A}) = -\frac{4\Delta_L^2}{\hat{D}} \sum_{i,\ell} (-1)^\ell \delta \hat{w}_i^{ab}[\ell] j_0^2(\Delta_L \Delta \hat{E}[\ell]), \quad (6)$$

TABLE IV. Effective $\delta \hat{w}_0^{e\mu}[\ell]/K_{1,2}^0$, Lower Transition. $K_{1,2}^0[\ell]$ is given in Table VI.

| Quantity | $\ell = 1$ | $\ell = 2$ | $\ell = 3$ |
|---|---|------------|--|
| $\delta \hat{w}_0^{e\mu}[\ell]/K_{1,2}^0$ | $-4\alpha R_p s_{23}^2 \tilde{A}(2(c_{12}^2 - R_p) - \tilde{A}(1 + s_{12}^2 + 2R_p))$ | 0 | $2\alpha \tilde{A} \hat{A} c_{12}^2 c_{23}^2 s_{12}^2$ |

TABLE V. Effective $\delta \hat{w}_{cos}^{e\mu}[\ell]/K_{1,2}^c$ Lower Transition $K_{1,2}^c[\ell]$ is given in Table VI.

| | $\delta \hat{w}_{cos}^{e\mu}[\ell]/K_{1,2}^c$ |
|------------|--|
| $\ell = 1$ | $1 - \alpha(1 + 2s_{12}^2 + R_p) - 2\hat{A}(1 - \alpha(1 + 2s_{12}^2 + R_p)) + \hat{A}^2(1 - \alpha(1 + 3R_p))$ |
| $\ell = 2$ | $-\frac{1}{\hat{A}^2}(1 - \alpha(1 + 2c_{12}^2 + R_p) + \hat{A}(2 - \alpha(1 + 2c_{12}^2 + 9R_p)) + \hat{A}^2(1 - \alpha(1 + 2c_{12}^2 + 3R_p)) + \alpha R_p \hat{A}^3)$ |
| $\ell = 3$ | $-\frac{1}{\hat{A}^2}(1 - \hat{C}_\alpha - \hat{A}(2 - \hat{C}_\alpha + \alpha(2 - 4c_{12}^2 - R_p)) + \alpha \hat{A}^2(5 - 8c_{12}^2 + 3R_p)) + \hat{A}^3(2 - \alpha(4s_{12}^2 + 9R_p)) \hat{A}^4(1 - \alpha(1 + R_p))$ |

TABLE VI. Definitions of $K_{1,2}^0[\ell]$ (Table IV) and $K_{1,2}^c[\ell]$ (Table V)

| Quantity | $\ell = 1$ | $\ell = 2$ | $\ell = 3$ |
|-------------------|--|--|--|
| $K_{1,2}^c[\ell]$ | $\alpha c_{12} s_{12} \sqrt{\alpha R_p}/2$ | $\alpha c_{12} s_{12} \sqrt{\alpha R_p}/2$ | $\alpha c_{12} s_{12} \sqrt{\alpha R_p}/2$ |
| $K_{1,2}^0[\ell]$ | $\alpha R_p s_{23}^2/\tilde{A}$ | $\alpha R_p s_{23}^2/\tilde{A}$ | $\alpha R_p s_{23}^2/\tilde{A}$ |

with $\delta \hat{w}_0^{e\mu}[\ell]$ given in Table IV and $\delta \hat{w}_{cos}^{e\mu}[\ell]$ in Table V. In Eq. (6), the sum over i runs over the two values $(0, cos)$. Note that the effective $\delta \hat{w}_0^{e\mu}[1] = 0$.

TABLE VII. $\hat{w}_0^{e\mu}[\ell]$ and $\Delta\hat{E}[\ell] = \Delta\hat{E}_0[\ell](1+r[\ell])$ Above Solar

| Quantity | | $\ell = 1$ | $\ell = 2$ | $\ell = 3$ |
|--------------------------|-------------|---|-------------|------------|
| $\hat{w}_0^{e\mu}[\ell]$ | | $-\frac{\alpha R_p}{\hat{C}_\alpha} s_{23}^2 (\hat{A}\tilde{A}^2 + \alpha(4R_p - \tilde{A}(s_{12}^2 + 8R_p))) + D\hat{w}_0^{e\mu}[1]$ | 0 | 0 |
| $\Delta\hat{E}_0[\ell]$ | Eq (9) (a) | Eq (9) (b) | Eq (9) (c) | |
| $r[\ell]$ | Eq (10) (a) | Eq (10) (b) | Eq (10) (b) | |

2. Above the Lower Transition Region

In all regions above the lower transition region, our simplified oscillation probability $P^{+ab}(\Delta_L, \hat{A})$ has just one component,

$$P^{+ab}(\Delta_L, \hat{A}) = \frac{4\Delta_L^2}{\hat{D}} (\hat{w}_0^{ab}[1] + D\hat{w}_0^{e\mu}[1]) j_0^2(\Delta_L \Delta\hat{E}[1]), \quad (7)$$

where the coefficient $\hat{w}_0^{e\mu}[1]$ is given in Table VII and the quantity $D\hat{w}_0^{e\mu}[1]$,

$$D\hat{w}_0^{e\mu}[1] = \frac{2\alpha^2 R_p^2}{\hat{C}_\alpha} s_{23}^2 (3c_{12}^2 + 4R_p), \quad (8)$$

is a correction required for accuracy in the atmospheric resonance region. The Bessel function in Eq. (7) simplified by using its expanded representation given in Eq. (17) below and taking $\Delta\hat{E}[1]$ from Table VII. We find,

$$P^{+ab}(\Delta_L, \hat{A}) = \frac{4\Delta_L^2}{\hat{D}} ((\hat{w}_0^{ab}[1] + D\hat{w}_0^{e\mu}[1]) j_0^2(\Delta_L \hat{C}_\alpha) + 2r[\ell] \hat{w}_0^{ab}[1] (j_0(2\Delta_L \hat{C}_\alpha) - j_0^2(\Delta_L \hat{C}_\alpha))), \quad (9)$$

where the term $r[\ell] D\hat{w}_0^{e\mu}[1]$ has been dropped because it is of order α^3 and therefore quite small. The short-hand notation $\tilde{A} \equiv 1 - \hat{A}$ is used in Table VII and below for the frequently occurring quantity $1 - \hat{A}$.

C. Simplifying $j_0^2(\Delta_L \Delta\hat{E}[\ell])$

The Bessel functions,

$$j_0(\hat{\Delta}[\ell]) \equiv j_0(\Delta_L \Delta\hat{E}[\ell]) \quad (10)$$

may be simplified when $\Delta\hat{E}[\ell]$ consists of two leading terms,

$$\Delta\hat{E}[\ell] = \Delta\hat{E}_0[\ell](1+r[\ell]), \quad (11)$$

as it does above the solar resonance region, and, in addition, $\Delta_L r[\ell] \Delta\hat{E}_0[\ell] \ll 1$. In this case, the trigonometric identity,

$$\begin{aligned} & \sin \Delta_L (\Delta\hat{E}_0[\ell] + r[\ell] \Delta\hat{E}_0[\ell]) \\ &= \sin \Delta_L \Delta\hat{E}_0[\ell] \cos \Delta_L r[\ell] \Delta\hat{E}_0[\ell] \\ &+ \cos \Delta_L \Delta\hat{E}_0[\ell] \sin \Delta_L r[\ell] \Delta\hat{E}_0[\ell], \end{aligned} \quad (12)$$

and the approximations,

$$\begin{aligned}\cos \Delta_L r[\ell] \Delta \hat{\hat{E}}_0[\ell] &\approx 1 \\ \sin \Delta_L r[\ell] \Delta \hat{\hat{E}}_0[\ell] &\approx \Delta_L r[\ell] \Delta \hat{\hat{E}}_0[\ell] ,\end{aligned}\tag{13}$$

allow us to write,

$$\begin{aligned}j_0(\Delta_L \Delta \hat{\hat{E}}[\ell]) &= \frac{1}{1+r[\ell]} j_0(\Delta_L \Delta \hat{\hat{E}}_0[\ell]) \\ &+ \frac{r[\ell]}{1+r[\ell]} \cos \Delta_L \Delta \hat{\hat{E}}_0[\ell] .\end{aligned}\tag{14}$$

In Eq. (14),

$$j_0(\Delta_L \Delta \hat{\hat{E}}_0[\ell]) \equiv \frac{\sin \Delta_L \Delta \hat{\hat{E}}_0[\ell]}{\Delta_L \Delta \hat{\hat{E}}_0[\ell]} .\tag{15}$$

Squaring Eq. (14) and retaining the first two leading terms, we find

$$j_0^2(\Delta_L \Delta \hat{\hat{E}}[\ell]) = \frac{1}{(1+r[\ell])^2} j_0^2(\Delta_L \Delta \hat{\hat{E}}_0[\ell]) + \frac{2r[\ell]}{(1+r[\ell])^2} j_0(\Delta_L \Delta \hat{\hat{E}}_0[\ell]) \cos \Delta_L \Delta \hat{\hat{E}}_0[\ell] .\tag{16}$$

The Bessel function may be simplified by expanding it to first order in $r[1]$,

$$\begin{aligned}j_0^2(\Delta_L \Delta \hat{\hat{E}}[\ell]) &= j_0^2(\Delta_L \Delta \hat{\hat{E}}_0[\ell]) (1 - 2r[\ell]) + 2r[\ell] j_0(2\Delta_L \Delta \hat{\hat{E}}_0[\ell]) \\ &= j_0^2(\Delta_L \Delta \hat{\hat{E}}_0[\ell]) + 2r[\ell] (j_0(2\Delta_L \Delta \hat{\hat{E}}_0[\ell]) - j_0^2(\Delta_L \Delta \hat{\hat{E}}_0[\ell])) .\end{aligned}\tag{17}$$

ACKNOWLEDGMENTS

We are indebted to Ernest Henley who introduced us to the subject of neutrino oscillations and made

important contributions to the present paper. LSK thanks LANL group P-25 for its support.

-
- [1] M. B. Johnson, E. M. Henley, and L. S. Kisslinger, Phys. Rev. **D91**, 076005 (2015).
 - [2] The ISS Working group, arXiv:0710.4947/hep-ph.
 - [3] L. Wolfenstein, Phys. Rev. **D17**, 2369 (1978).
 - [4] S. P. Mikheev and A. Yu. Smirnov, Soviet Journal Nuclear Physics 42, 913-917 (1985).
 - [5] R. Davis Jr., Phys. Rev. Lett. 12, 303-305 (1964).
 - [6] B.T. Cleveland et al., Astrophys. J. 496, 505-526 (1998).
 - [7] Irina Mocioiu and Robert Shrock, Phys. Rev. **D62**, 053017 (2000).
 - [8] M. Freund, Phys. Rev. **D64**, 053003 (2001).
 - [9] E. Akhmedov, P. Huber, M. Lindner, and T. Ohlsson, Nucl. Phys. **B608**, 394 (2001).
 - [10] M. Jacobson and T. Ohlsson, Phys. Rev. **D69**, 013003 (2004).
 - [11] M. B. Johnson, E.M Henley, and L. S. Kisslinger, arXiv:1507.07836/hep-ph (2016).
 - [12] Zhi-zhong Xing, Phys. Lett. B 487, 327 (2000); Phys. Rev. D 64, 073014 (2001).
 - [13] E. M. Henley, M. B. Johnson, and L. S. Kisslinger, Int J. Mod Phys. E **20**, 2463 (2011); arXiv:1102.5106/hep-ph (2011).
 - [14] L. S. Kisslinger, E. M. Henley, and M. B. Johnson, arXiv:1105.2741/hep-ph (2011).
 - [15] H. Davoudiasl, H. S. Lee, and W. J. Marciano, Phys. Rev. **D84**, 013009, (2011).
 - [16] M. C. Gonzalez-Garcia, M. Maltoni, and J. Salvado, arXiv:1103.4365/hep-ph; JHEP 1105: 075 (2011).
 - [17] F.P. An et.al., Daya Bay Collaboration, Chin. Phys. C37, 01101 (2013); arXiv:1210.6327/hep-ex.
 - [18] V. Barger, K. Whisnant, S. Pakvasa, and R. J. N. Phillips, Phys. Rev. **D22**, 2718 (1980).
 - [19] L. S. Kisslinger, Int J. Mod Phys. A **28**, 1350153 (2013); arXiv:1211.3348/hep/ph.